

Review

Safety Issues of Layered Nickel-Based Cathode Materials for Lithium-Ion Batteries: Origin, Strategies and Prospects

Zhongfeng Tang ^{1,*}, Dandan Feng ^{2,3}, Yali Xu ¹, Lei Chen ¹, Xiangdan Zhang ¹ and Qiang Ma ¹

¹ Henan International Joint Laboratory of Rare Earth Composite Materials, College of Materials Engineering, Henan University of Engineering, Zhengzhou 451191, China

² College of Chemical Engineering and Food Science, Zhengzhou University of Technology, Zhengzhou 450044, China

³ Postdoctoral Innovation Practice Base, Zhengzhou Institute of Technology, Zhengzhou 450044, China

* Correspondence: tangzf@haue.edu.cn

Abstract: Layered lithium transition metal (TM) oxides LiTMO₂ (TM = Ni, Co, Mn, Al, etc.) are the most promising cathode materials for lithium-ion batteries because of their high energy density, good rate capability and moderate cost. However, the safety issue arising from the intrinsic thermal instability of nickel-based cathode materials is still a critical challenge for further applications in electric vehicles and energy storage power stations. The main reasons include side reactions between the highly reactive Ni^{3+/4+} and liquid electrolyte, oxygen release accompanied by structural phase transition, and internal microcrack propagation owing to the low strength of spherical secondary particles. Great efforts have been invested to modify nickel-based cathode materials such as stabilization of bulk structure by element doping, surface engineering, nanostructure design, and particle mono-crystallization. In this review, we summarize these advances and try to give an in-depth insight into the origin of the thermal instability of nickel-based cathode materials. More importantly, some effective strategies to improve thermal stability are outlined, expecting to accelerate the future development of layered TM oxides with high safety.



Citation: Tang, Z.; Feng, D.; Xu, Y.; Chen, L.; Zhang, X.; Ma, Q. Safety Issues of Layered Nickel-Based Cathode Materials for Lithium-Ion Batteries: Origin, Strategies and Prospects. *Batteries* **2023**, *9*, 156. <https://doi.org/10.3390/batteries9030156>

Academic Editors: Xijun Xu, Zhuosen Wang, Ling Kang and Carolina Rosero-Navarro

Received: 22 January 2023

Revised: 22 February 2023

Accepted: 27 February 2023

Published: 1 March 2023



Copyright: © 2023 by the authors. Licensee MDPI, Basel, Switzerland. This article is an open access article distributed under the terms and conditions of the Creative Commons Attribution (CC BY) license (<https://creativecommons.org/licenses/by/4.0/>).

Keywords: lithium-ion batteries; layered lithium transition metal oxides; safety; thermal instability; oxygen release; coating; doping

1. Introduction

Lithium-ion batteries have become the market leader in portable electronic devices (such as smartphones and laptops) due to their high energy density, long cycle life, low self-discharge rate, and reduced cost [1–3]. This rechargeable battery laid the foundation of a wireless and portable lifestyle as the Nobel Prize in Chemistry 2019 said [4]. From a clean energy perspective, electric cars using lithium-ion batteries are becoming increasingly popular, and large-scale energy storage power stations are being widely constructed jointly with wind or photovoltaic power generations [5].

Basically, a lithium-ion battery (cell) is composed of cathode (positive) material, anode (negative) material, separator, electrolyte, and other auxiliary materials, such as a binder, current collector, lug and shell. In commercial lithium-ion batteries, the practical capacity of cathode material determines the upper limit of the battery energy density given the fact that graphite still dominates the anode electrode today. The commercialized cathode materials include layered structure materials, spinel type materials (LiMn₂O₄ for example), and olivine type materials (LiFePO₄ for example). As shown in Table 1, the layered Ni-based cathode materials have good comprehensive performance, such as high energy density, good cycle performance, and moderate cost [6]. Compared to LiFePO₄ (~150 mAh g⁻¹) and LiMn₂O₄ (~110 mAh g⁻¹), the layered nickel-based materials, such as LiNi_{0.5}Co_{0.2}Mn_{0.3}O₂ (NCM523), LiNi_{0.8}Co_{0.1}Mn_{0.1}O₂ (NCM811) and LiNi_{0.8}Co_{0.15}Al_{0.05}O₂ (NCA), are taking the market share of power battery because of their higher capacity (>165 mAh g⁻¹) [7].

Table 1. A comparison of several commercial cathode materials.

Cathode	Specific Capacity (mAh g ⁻¹)		Voltage (V)	Energy Density * (Wh kg ⁻¹)	Cycle Life	Cell Material Cost * (USD kWh ⁻¹)	Safety
	Theoretical	Practical					
LiCoO ₂	275	140	3.7	150~200	~1000	>120	poor
LiMn ₂ O ₄	140	110	3.9	215	~800	~76	good
NCM (Ni < 60%)	273	165	3.65	~250	>2500	81~88	medium
Ni-rich	273	>200	3.65	~300	~2000	72~74	poor
LiFePO ₄	170	150	3.3	~210	~5000	~85	excellent

* Note: data reproduced from ref. [6].

However, safety accidents (such as smoke and fire), hundreds for electric cars, and scores for energy storage power stations, have been reported every year worldwide, most of which were caused by the thermal runaway of lithium-ion batteries according to the investigation reports [2,8–10]. Therefore, it's necessary to figure out the main reasons behind the thermal runaway of lithium-ion batteries.

At present, the mechanism and failure sequence of battery thermal runaway have been deeply studied. It is generally believed that under the conditions of mechanical abuse, electrical abuse, and heat abuse, an irreversible temperature rise occurs inside the battery, which then leads to a series of exothermic side reactions such as separator melting, short circuit, and cathode material decomposition, and finally leads to thermal runaway of the battery [11]. Based on the results of hundreds of accelerating rate calorimetry (ARC) tests with various types of batteries (including cylinder, prismatic, and pouch cell), three temperatures, {T₁, T₂, T₃}, were clearly observed and summarized as the common characteristics of battery thermal runaway [12,13]. T₁ represents the onset temperature of abnormal heat generation mainly attributed to the decomposition of the solid electrolyte interface (SEI), reflecting the overall thermal stability of a battery cell. T₁ is usually observed between 70~150 °C, relating to the composition of electrolytes and aging conditions. Notably, the growth of lithium dendrites during cycling at a low temperature can significantly decrease T₁ and may pierce the holes of the separator. T₂ is the triggering temperature of battery TR, i.e., the tipping point that separates the gradual temperature increase and the sharp temperature rise. The temperature rise rate, dT·dt⁻¹, can exceed 1 °C·s⁻¹ when reaching T₂, with separator melting, short circuit, and decomposition of cathode materials. T₃ is the maximum temperature that can be reached after the battery is out of control, which is directly related to the type and capacity of the cell and affects the heat spread rate in the battery pack. In the above three stages, the process of the internal temperature rising from T₁ to T₂ is the key period for the battery management system (BMS) to be able to conduct safety identification, early warning, and active intervention management, which can provide a certain time for personnel escape and fire-fighting. When the cell temperature reaches T₂, it is basically out of control, and can reach the combustion state in a short time. It can only rely on system-level passive protection measures to prevent the further heat spread of the battery pack. Therefore, it's very important to inhibit or slow down the reaction and heat release in the cell at T₁ and T₂ stages to prolong safety warning time and reduce personnel and property losses.

In a word, the thermal/chemical stabilities of liquid electrolytes, anode/cathode materials and separators are all related to the safety of lithium-ion batteries, and many ideas have been proposed accordingly to improve the safety of lithium-ion batteries [14]. While during this process, the decomposition of delithiated cathode materials indicates the accelerated stage of thermal runaway with a temperature rise over 1°C min⁻¹ inside the battery and a sharply drop in voltage [13,15]. Clearly, the cathode materials play a critical role in ensuring the batteries' reliability. Indeed, different cathode materials greatly affect the severity of safety accidents. Batteries using LiFePO₄, one of the most commonly used cathode materials in electric cars, might only smoke when thermal runaway occurs, while those involving layered LiTMO₂ materials always end with fire, deflagration, and even

explosion [16–18]. The main reasons for these differences will be discussed in more detail in the following sections.

Herein, we focus on the safety issue of nickel-based cathode materials from the aspects of composition, structure, and chemical stability, and try to give an in-depth insight into the origin of thermal instability in Section 2. Then Section 3 summarizes the advances and the strategies to improve the thermal stability of layered LiTMO₂ materials. Finally, some conclusions and perspectives are provided in Section 4.

2. Thermal Stability of Layered LTMO₂

The thermal stability of layered LiTMO₂ materials is influenced by multiple factors, mainly including composition, structure, and morphology as well as chemical activity. Specifically, the onset temperature of decomposition, exothermic reaction peak temperature, total enthalpy, and decomposition products are important evaluation parameters for the thermal stability of electrode materials [19].

2.1. Composition

Layered lithium transition-metal oxides have a common chemical formula LiTMO₂ (TM = Ni, Co, Mn, Al, etc.), in which TM representatives one or more of the transition metals. LiCoO₂ is the most widely used cathode material in electronic devices because of its easy synthesis process, stable electrochemical performance, and highest compaction density [20,21]. However, the high cost and toxicity of cobalt make it unsuitable for electric vehicles and other large applications. LiNiO₂ is another promising layered cathode material with a similar theoretical specific capacity of 274 mAh g⁻¹ vs. LiCoO₂ (275 mAh g⁻¹), while the practical specific capacity of LiNiO₂ (>220 mAh g⁻¹) is much higher than that of LiCoO₂ (~160 mAh g⁻¹) below 4.3 V [22]. Unfortunately, it's very difficult to synthesize a pure LiNiO₂ since lithium vacancies, cation disordering, and spinel phase are easier to form in the sintering process [23].

As mentioned before, single transition metal oxide (such as LiCoO₂ and LiNiO₂) cannot meet the increasing requirements of the battery market due to various deficiencies. Ternary cathode materials, especially LiNi_xCo_yMn_zO₂ (x + y + z = 1), have attracted great attention since 1999 when Liu first proposed a co-substitution of Ni by Co and Mn in LiNiO₂ [24]. Nickel, Cobalt, and Manganese are randomly and uniformly distributed in the transition metal layer with performing their own functions, i.e., Ni for capacity, Co for layered characteristics, and Mn for stability. The synergistical effect of the three elements significantly improves the electrochemical performance of NCM and makes it a very successful commercial cathode material. In recent years, nickel fraction in commercial NCM materials has exceeded 60% in order to pursue higher energy density, which is called Ni-rich materials, such as NCA, NCM811 and LiNi_{0.89}Co_{0.05}Mn_{0.05}Al_{0.01}O₂ (NCMA) [15,25,26]. Besides, the rapidly rising cost of cobalt also promotes the development of cobalt-free Ni-rich cathode materials (LiNi_{0.883}Mn_{0.056}Al_{0.061}O₂ for example).

However, the biggest challenge for Ni-rich materials is how to balance the contradiction between high energy density and reduced thermal stability. It's well known that the thermal stability of layered LiTMO₂ materials strongly depends on their composition, especially the Ni content, i.e., the higher the Ni content, the lower the stability. As shown in Figure 1a, Noh [27] compared the thermal stability of delithiated NCM materials with different nickel contents and found that the exothermic peak temperature drastically decreased from 306 °C to 225 °C for Li_{0.37}Ni_{1/3}Co_{1/3}Mn_{1/3}O₂ and Li_{0.21}Ni_{0.85}Co_{0.075}Mn_{0.075}O₂ respectively, while the heat generation significantly increased from 512.5 J g⁻¹ to 971.5 J g⁻¹. These differences can be attributed to the varied valence with different Ni content. According to the results of in situ time-resolved X-ray diffraction and mass spectroscopy (TR-XRD/MS), Bak et al. schematically depicted the phase stability map of the charged NMC cathode materials during heating (Figure 1b), which also clearly showed that the thermal stability of the charged NCM samples decreases with increasing Ni content [28]. Further study shows that the average valence of Ni increases from +2 to +3 with the in-

creasing Ni content, while Ni^{3+} -TM bond strengths decrease and Ni^{3+} -O bonds become increasingly covalent, leading to the intrinsic thermodynamical instability of the layered structure [29].

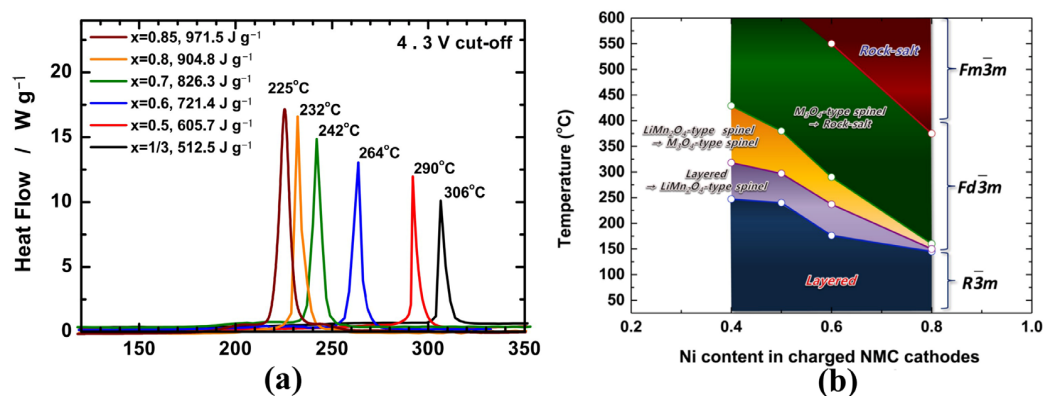


Figure 1. (a) DSC results of the $\text{Li}_{1-\delta}[\text{Ni}_x\text{Co}_y\text{Mn}_z]\text{O}_2$ materials ($x = 1/3, 0.5, 0.6, 0.7, 0.8$ and 0.85) [27]; (b) Schematic illustration depicting the phase stability map of the charged NMC cathode materials during heating [28].

2.2. Structure and Morphology

All of the layered LiTMO_2 compounds correspond to a hexagonal $\alpha\text{-NaFeO}_2$ structure with the $\text{R}\bar{3}\text{m}$ space group. Specifically, oxygen atoms form a cubic close-packed lattice with rhombohedral distortion along the c -direction, resulting in layers formed by edge-sharing octahedra sites which are occupied by transition metals (3a) and lithium (3b) alternately [30]. But there is a common problem in layered nickel-based cathode materials named $\text{Li}^+/\text{Ni}^{2+}$ anti-site defects or cation disordering which mainly result from their similar ionic radii (Li^+ : 0.072 nm, Ni^{2+} : 0.069 nm) [31]. These disordering occupations hinder the Li^+ diffusion in the two-dimensional channels and greatly affect the electrochemical performance. Besides that [32], the distribution of TM ions inside the layer is no longer uniform, but the minority of TM ions form clusters at the atomic level when Ni content exceed 80%. The clusters make Mn^{4+} reduce to Mn^{3+} , leading to aggravating Jahn–Teller distortions. These atomic-level structure deficiencies weaken the TM–TM interactions and TM–O bonds, thus significantly affecting the thermal stability of nickel-based materials.

In the delithiation process, the structure phase converts from hexagonal (H1) over monoclinic (M) to hexagonal (H2 and H3) phases, and the phase transitions reverse in the discharging process [33–35]. With the increase of lithium vacancy in the charging process, the distortion of TM–O octahedra gradually increases along the c -axis direction. As shown in Figure 2, when the amount of lithium removal exceeds the threshold (depending on the nickel content and charging cutoff voltage), parts of the region (H3 phase) cannot remain the layered characteristic anymore and convert to spinel Ni_3O_4 with active oxygen release [35]. The H2 to H3 phase transition usually occurs at a high delithiated state and results in oxygen evolution, which is also one of the main reasons for thermal runaway caused by overcharge [18]. With regard to the thermal decomposition under abusive conditions, the delithiated layered LiTMO_2 materials go through phase transitions from layered structure to the disordered spinel structure, and finally to the rock-salt structure, accompanied by a large amount of oxygen gas release and CO_2 formation [35,36]. Noted that the oxygen gas release occurs around 200 $^\circ\text{C}$, at which the electrolyte has been decomposed or oxidized into combustible gas. As we all know, oxygen is the most common combustion promoter among the three elements of combustion. Therefore, batteries using layered LiTMO_2 materials always catch fire or even explode when thermal runaway happens. Similarly, layered oxides like LiCoO_2 and Mn-based Li-rich cathode materials also have the common problem of oxygen release. Samsung’s Galaxy Note 7 explosion strongly indicates that LiCoO_2 battery with design defects may cause serious accidents. In contrast, the dilithiated LiFePO_4 remains

quite stable even above 350 °C and with little oxygen release, thus the weaknesses of the LiFePO_4 battery are the separator and electrolyte rather than the cathode material.

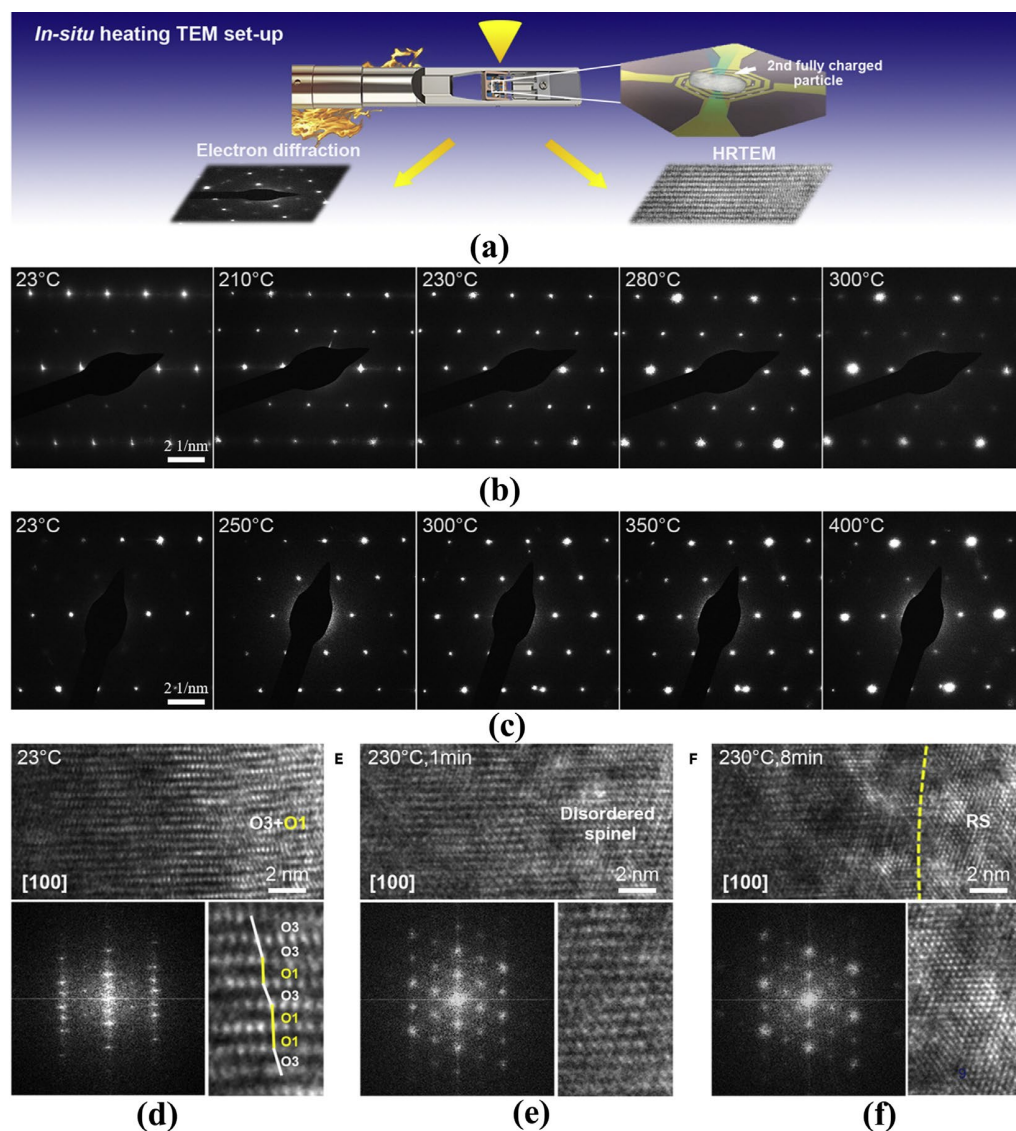


Figure 2. In situ structural evolution of delithiated LNO and doped LNO induced by oxygen loss. (a) Schematic illustration of the in-situ heating TEM experimental setup. (b,c) Time-resolved EDPs of LNO (b) and doped LNO (c) during in situ heating at different temperatures. (d–f) Time-resolved HRTEM images showing structural transformations of delithiated LNO from layered structure (O3) with O1 phases (d) to disordered spinel (e) and then to rock-salt structure (f) induced by oxygen loss during in situ heating. The lower panels show corresponding fast Fourier transforms and enlarged images of local regions. O3 and O1 phases are indicated by white and yellow lines, respectively [35].

The particle microstructures and morphologies also play an important role in influencing the electrochemical properties and thermal stability of electrode materials. For commercial Ni-based materials, the spherical precursors are firstly agglomerated by nano-sized primary crystals with random orientations and a large number of defects in the coprecipitation process. Then the subsequent high-temperature treatment makes nanocrystals grow up and poly-crystallization, which means many crystal defects, such as grain boundaries, still exist inside the particle [23]. As shown in Figure 3a, the resulting unbalanced mechanical stress inside the particles during the charge-discharge process can cause microcracks that weaken the structural stability of particles and aggravate the undesired cathode-electrolyte side reactions [37–40]. In particular, the particles in at highly delithiated

state may smash at high temperatures and accelerate side reactions and oxygen release (Figure 3b–d) [36].

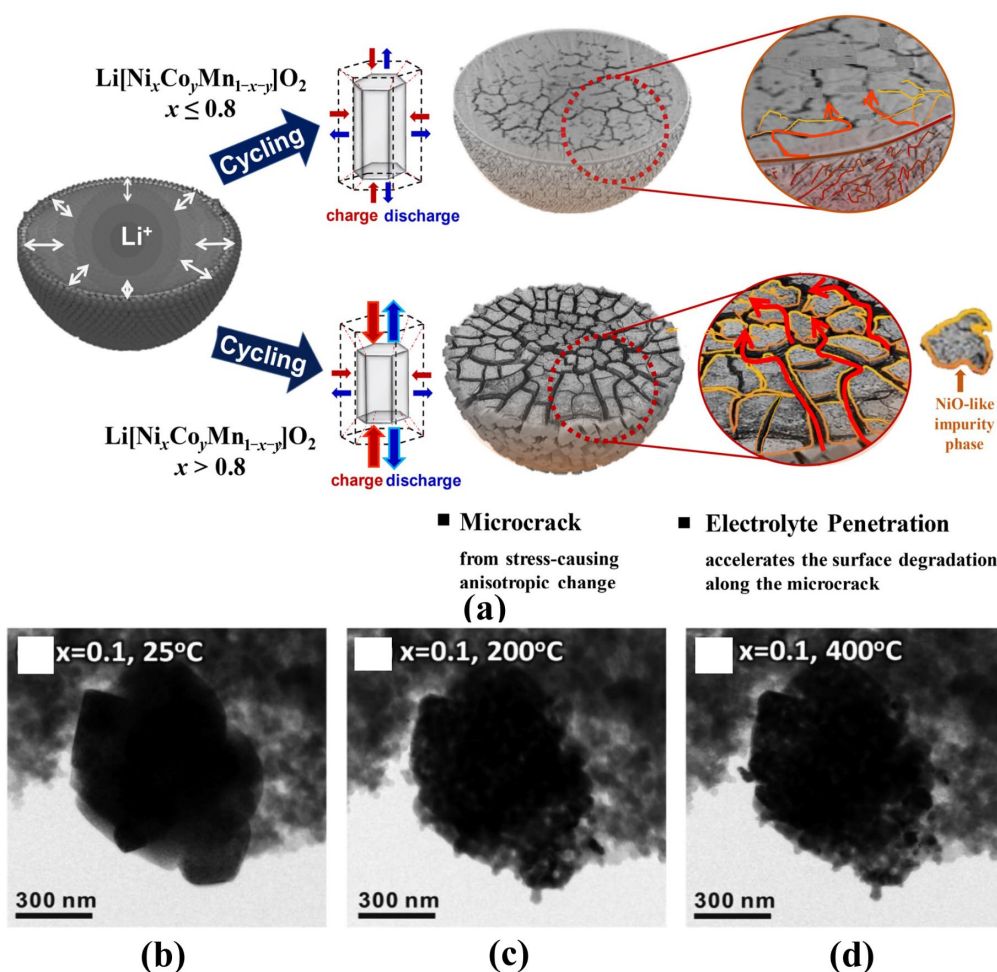


Figure 3. (a) Scheme of microcrack generation and electrolyte penetration [37]. In situ TEM images (b) before heating (25 °C), after heating at (c) 200 °C, and (d) 400 °C for a $\text{Li}_{0.1}\text{Ni}_{0.8}\text{Co}_{0.15}\text{Al}_{0.05}\text{O}_2$ particle [36].

2.3. Chemical Activity

The chemical activity of electrode materials is directly related to the gas production inside the battery. Because of the different out shell electron configurations for Ni and Co, the $\text{Ni}^{2+}/\text{Ni}^{3+}/\text{Ni}^{4+}$ redox contributes to most of the capacity of Ni-based materials below 4.3 V (vs. Li/Li^+) while $\text{Co}^{3+}/\text{Co}^{4+}$ redox occurs at around 4.3 V in the charging process [41]. However, the highly active Ni^{4+} on the particle surface can easily be reactive with liquid electrolytes accompanied by the gas generation (mainly including CO_2 and CO) [42,43]. Secondly, the lithium residues (such as Li_2CO_3 and LiOH) introduced in the synthesis process or by-products of the slow reduction of Ni^{3+} to Ni^{2+} for Ni-rich materials when exposed to moisture, can also induce gas generation inside the battery [44,45]. Finally, transition metals (especially Mn) can slowly dissolve into the electrolyte, then migrate and incorporate into solid electrolyte interphase (SEI) film of the graphite-based negative electrode, resulting in the damage of SEI and continues alkane gas evolution [46,47]. Actually, the gas evolution related to the chemical activity of electrode materials is a common phenomenon of battery failure, which makes the battery bulge and leakage, and causes safety problems.

In summary, the thermal instability of layered LiTMO_2 materials attributes to: (1) compositions, specifically, the higher the Ni content, the worse the thermal stability;

(2) oxygen release from delithiated materials due to the phase transitions under over-charge or heated conditions; (3) gas evolution caused by the highly oxidative Ni^{4+} , lithium residues, and transition metals dissolution. Nevertheless, the core reason is the oxygen release due to the unstable layered structure of delithiated LiTMO_2 materials under abusive conditions. Therefore, the key to improving the safety of LiTMO_2 batteries is to reduce or delay oxygen release by improving the structural stability of materials, and we will summarize the advances and strategies in the following sections.

3. Safety Strategies for Ni-Based Cathode Materials

With the deepening understanding of the thermal failure mechanism of layered Ni-based materials, corresponding modification measures have been put forward. Great efforts have been devoted to improving the thermal stability of cathode materials from surface to the inside, such as elements doping, surface coating, microstructure design, morphology control, and so on.

3.1. Elements Doping

A lot of experimental and theoretical studies have shown that element doping can effectively stabilize the material structure. Generally speaking, the main role of elements doping or substitution is to prop up the layered structure after the removal of lithium (named pillar effect) so as to prevent or slow down the phase transitions of LiTMO_2 . According to the different doping sites, it can be classified into cation doping, anion doping, and co-doping. Specifically, cations usually occupy the TM sites or lithium sites, and anions substitute for the oxygen.

High valence cations, such as Al^{3+} , Ti^{4+} , Zr^{4+} , W^{5+} , V^{5+} , Mo^{6+} and Nb^{5+} , have been fully studied as dopants in the TM layer [48–56]. Levartovsky [49] conducted a comparative study of Al and Ti doping in $\text{LiNi}_{0.85}\text{Co}_{0.1}\text{Mn}_{0.05}\text{O}_2$ (NCM85), which indicated that both Al and Ti can improve the thermal stability with a close onset temperature of 214 °C, 216 °C and 218 °C, but with a significantly decreased specific total heat release of 468 J g^{-1} , 376 J g^{-1} and 352 J g^{-1} for NCM85 pristine, Ti-doped and Al-doped samples, respectively (Figure 4). It may ascribe to their strong bonds with O and the construction of a protective layer that can reduce oxygen release, while the authors also acknowledge that the relevant mechanism is still unclear. Similarly, the strong W-O bond makes the average charge around O in the NiO_6 octahedron more negative, which can effectively suppress the oxygen evolution and thus improve the thermal stability of Ni-based cathode materials [53]. Theoretical studies using first-principles density functional theory (DFT) calculations show that, after high valence cations doping, the more stable Ni^{2+} state is preferred to Ni^{3+} or Ni^{4+} because of the charge compensation, and oxygen vacancies are prevented [28]. In addition, the different doping sites in the TM layer also have different effects, i.e., doping at Mn sites (It may be more accurate to call it substitution) reduces Li/Ni disordering and oxygen release, while doping at Co sites improves the phase stability [57].

The low valence cations, mainly including Na^+ [58–62] and Mg^{2+} [63,64], are generally believed that they can enter the lithium layer as inactive pillars. Na^+ doping can significantly improve the electrochemical performance of Ni-based cathode materials, but there is little research on the improvement of thermal stability. A few studies show that Mg^{2+} , with a radius (0.072 nm) similar to that of Li (0.076 nm), can stabilize the lithium layer as an effective pillar and thus shift the onset of the exothermic reaction and phase transition toward higher temperature [63]. Interestingly, some investigations indicated that $\text{Li}^+/\text{Ni}^{2+}$ cation mixing, i.e., Ni^{2+} doping in the lithium site, can also improve the thermal stability of Ni-based materials to some extent due to the stronger bonds between Ni^{2+} -O than that of Li^+ -O [50]. Clearly, the lithium sites doping to promote the thermodynamic stability of Ni-based materials prefer +2 ions to +1 ions.

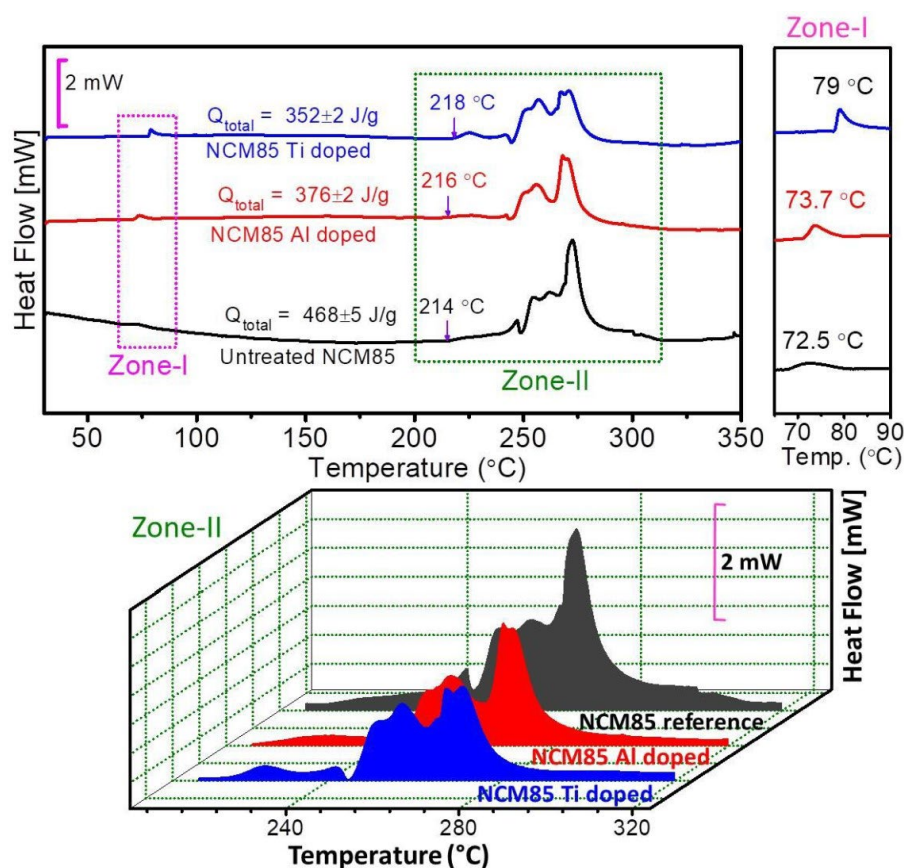


Figure 4. DSC measurements of NCM85 reference, Al-doped and Ti-doped cathode materials with electrolyte [49].

Anions, especially fluoride elements, have also been widely studied as doping elements to substitute oxygen partially in Ni-based cathode materials because of their similar chemical properties to oxygen ions. The reported fluoride sources include lithium fluoride (LiF) [65,66], ammonium fluoride (NH₄F) [67,68], polytetrafluoroethylene (PTFE) [69], polyvinylidene fluoride (PVDF) [70], lithium hexafluorophosphate (LiPF₆) [71], and so on. Typically, the fluorinated Li_{1-x}Ni_{0.8}Co_{0.1}Mn_{0.1}O_{2-z}F_z using NH₄F as a fluoride source showed greatly improved thermal stability with an exothermic peak temperature of 245 °C and a total generated heat of 1304 J g⁻¹ when z = 0.06, while the pristine Li_{1-x}Ni_{0.8}Co_{0.1}Mn_{0.1}O₂ had a broadening exothermic peak around 220 °C and a large generated heat of 3285 J g⁻¹ [68]. Similarly, a small amount of fluoride substituted Li_{1-x}Ni_{0.43}Co_{0.22}Mn_{0.35}O_{1.92}F_{0.08} exhibited a higher onset decomposing temperature of 280 °C and a reduced generated heat of 350 J g⁻¹, and those of the pristine sample were 236 °C and 590 J g⁻¹, respectively [66]. The positive effect of fluoride doping on the thermal stability of layered cathode was also observed in manganese-based Li-rich materials [65]. The strong O-F bonds can effectively stabilize the host layered structure and suppress the oxygen evolution at elevated temperatures. Thus, the thermal side reactions between these active oxygen species and the liquid electrolyte can be restarted [72].

Although single ion doping has been widely studied or applied in industrial production with varying degrees of improvement on the structural stability of cathode materials, it is still not enough to significantly improve battery safety. Multi-ion doping using two or more different ions seems to show better properties due to the synergistic effects theoretically. Ti⁴⁺ and F⁻ co-doping was conducted in Ni-rich material NCM811, which can induce the formation of an ultra-thin rock-salt phase that acts as a protective layer on the cathode surface and suppress the irreversible phase transition of H2 to H3, alleviating the structural degradation and thus improving the structural stability [73]. Other combinations, such as

Ti-B [74], Ti-Mg [75], Na-Mg [76], Ga-Zr [77], Nb-F [78], and K-Cl [79], are also investigated to improve the electrochemical properties, while the promotions in thermal stability are still lacking.

3.2. Surface Coating

The highly oxidative $\text{Ni}^{3+}/\text{Ni}^{4+}$ ions on the surface of Ni-based cathode materials, especially at a high delithiated state, can easily react with the liquid electrolyte and induce gas generation, which is one of the main reasons for the safety issues of batteries. The surface coating is like putting a protective layer on the particle surface to reduce the direct contact between the active material and the electrolyte, and thus suppress the side reactions and transition metals dissolution.

Generally speaking, the widely studied coating materials mainly include inactive compounds and conductive materials. The inactive compounds, such as oxides, fluorides, and phosphates, just play the role of a physical protective layer and barely involve chemical reactions. While conductive materials with lithium or electron conductivity, including lithium metal compounds, ionic conductors and electron conductive species, can not only stabilize the cathode interface but also facilitate lithium ions diffusion and electron transfer, improving the electrochemical properties [80]. The electron conductive materials, however, are more suitable for electrochemical properties improvement than thermal stability promotion according to current research. Below we will focus on the improvement of the thermal stability of Ni-based cathode with different coating materials and strategies.

A lot of inactive compounds, such as Al_2O_3 [81–84], TiO_2 [85–88], ZrO_2 [89], MgO [90,91], AlF_3 [92], AlPO_4 [93], Gd_2O_3 [94] and so on, can be used as coating materials for the layered cathodes. Among them, Al_2O_3 is one of the most successful coating materials and has been used in industrialization. NCM523 coated with a uniform Al_2O_3 layer of a thickness of about 9 nm by a simple wet chemistry method using $\text{Al}(\text{NO}_3)_3$ as an aluminum source showed a delayed exothermic peak at 444.9 °C and a lower generated heat of 257.5 J g^{-1} , while the bare sample had an exothermic peak with heat generation of 314.2 J g^{-1} at 430.4 °C [81]. In another study, NCM523 was coated with an ultrathin (~1.65 nm) Al_2O_3 layer by atomic layer deposition (ALD) method, delaying the exothermic peak from 355 °C to 367 °C after 20 charge-discharge cycles (Figure 5) [83]. Similarly, the TiO_2 coating layer can isolate the active oxygen species from electrolytes and postpone the phase transformation, thus slowing down parasitic oxidation and significantly improving battery safety. AlF_3 [92] and MnPO_4 [95] coating can also obviously improve the thermal stability of Ni-based cathode materials.

From the aspect of thermal improvement mechanism, the inactive coating layer mainly has the following functions: (a) acting as an isolation layer that reduces the harmful side reactions between the oxidative ions and electrolyte; (b) suppressing the phase transition near the surface and slowing down oxygen release; (c) preventing the cathode from HF or moisture attacking, i.e., HF scavenger [83]. It is worth noting that most inactive material coatings (especially metal oxides and fluoride) need to undergo high-temperature treatment, and element diffusion cannot be avoided. Therefore, the inactive materials coating is not only a single surface protective layer, but also has different levels of surface region doping [88]. In addition, the inert coating layer will hinder the rapid removal of lithium ions to a certain extent, and especially affect the rate performance of the battery. Therefore, the thickness, continuity, and uniformity of the coating layer need optimization to further improve the thermal stability of layered cathode materials.

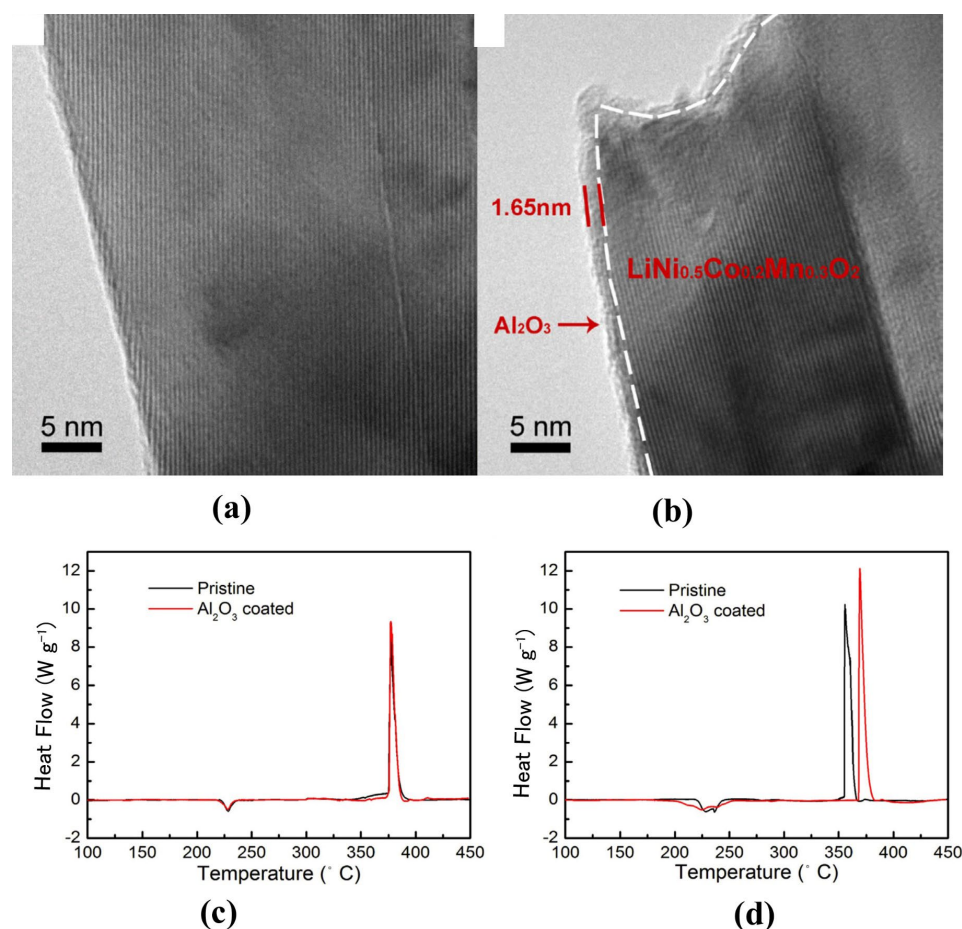


Figure 5. HRTEM images of NCM523 particles before (a) and after (b) Al_2O_3 ALD coatings, and DSC curves of the sealed pan with pristine or Al_2O_3 coated electrode material and electrolyte (c) 1st charged to 4.8 V and (d) Charged to 4.8 V after 20 cycles [83].

Lithium-ion conductors, including lithium metal oxides (such as Li_2TiO_3 , LiAlO_2 , and Li_2ZrO_3) [96–99], solid electrolytes (such as Li_3PO_4 , $\text{Li}_{1.3}\text{Al}_{0.3}\text{Ti}_{1.7}\text{PO}_4$ (LATP) and Li-La-TiO_3 (LLTO)) [100–104] and some stable cathode materials (such as LiFePO_4 and LiMnPO_4) [105–108] are more promising coating candidates to promote the thermal stability of layered Ni-based materials without sacrificing too much electrochemical performance. For example, Gan et.al. coated NCM811 with a 4–5 nm Li_3PO_4 layer through a solvent-free in-situ strategy, and identified, using atomic-scale microscopy, ex-situ SXAS, and in-situ Raman, that the Li_3PO_4 layer can effectively suppress NCM811 phase transition from a layered structure to a rock-salt-like structure and inhibit surface oxygen release [100]. Unfortunately, the sintering temperatures of most solid electrolytes (about 1000 °C or higher) differ significantly from that of layered Ni-based cathode materials (700–900 °C), which makes it difficult to prepare the expected phase of a target solid electrolyte when coating the host materials through a co-sintering method because of the inter diffusion of elements. Another interesting finding is that nano-sized LiFePO_4 can be prone to industrialization because of its excellent thermal stability and easy coating method. Typically, the nano-sized LFP particles and NCM spheres are fully mixed through mechanical fusion, forming a continuous LFP coating layer. The thermodynamic stable LFP can effectively protect the active Ni ions from the liquid electrolyte and reduce heat generation. Especially, as tested in 18,650 full batteries by ARC, the time between trigger temperature T_0 and the onset temperature T_c of thermal runaway is extended from 796 min to 989 min [105]. The extended time is quite important for early warning when battery safety issues are about to happen.

Evolved from the simple surface coating, Sun and coworkers first proposed and designed the concentration gradient materials, including core-shell structure with concentration gradient (CSG) [109], full concentration gradient (FCG) [110], and two-sloped full concentration gradient (TSFCG) [111]. There is also a lot of research to follow up on the technology [112–115]. Typically, as shown in Figure 6, the active Ni concentration decreases while the inactive Mn concentration increases linearly from the inside to the outside of the particles. The thermally stable Mn-rich layer can effectively protect the electrochemically active Ni-rich region from the harmful side reactions and phase transitions related to oxygen release, significantly shifting the exothermic peak from 221 °C to 257 °C for FCG $\text{LiNi}_{0.75}\text{Co}_{0.10}\text{Mn}_{0.15}\text{O}_2$ and $\text{LiNi}_{0.86}\text{Co}_{0.1}\text{Mn}_{0.04}\text{O}_2$ respectively [110].

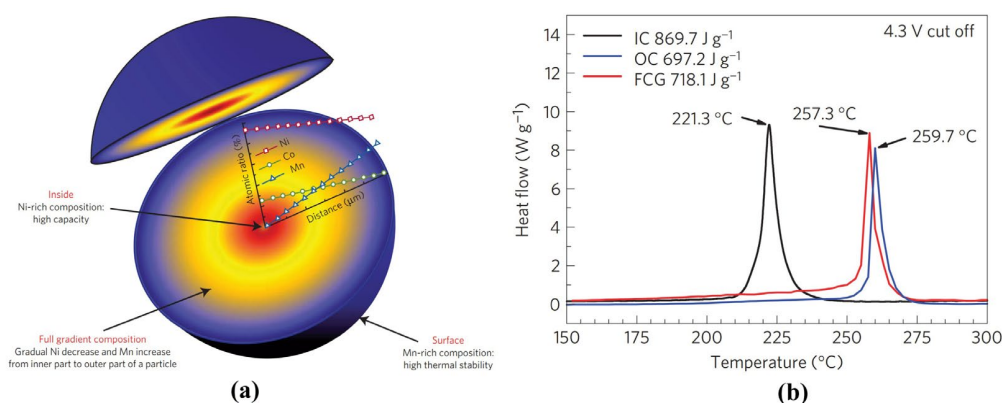


Figure 6. (a) Schematic diagram of the FCG lithium transition-metal oxide particle; and (b) DSC profiles of the delithiated FCG material, the delithiated inner composition (IC, $\text{Li}_{1-x}\text{Ni}_{0.86}\text{Co}_{0.10}\text{Mn}_{0.04}\text{O}_2$) and the delithiated outer composition ($\text{Li}_{1-x}\text{Ni}_{0.70}\text{Co}_{0.10}\text{Mn}_{0.2}\text{O}_2$) with a scanning rate of 1 °C min⁻¹ after charging to 4.3 V [110].

In short, the surface coating has been proven to be an effective improvement technology in both research and industry. The continuity and thickness of the coating layer, interface interaction between the coating material and host material, and properties of coating materials deserve more attention in order to more effectively inhibit the phase transition of the layered structure and slow down the release of oxygen. Similar to co-doping, the combination of multiple coating materials is also a promising research area [82,116–118].

3.3. Particle Microstructure Design

At present, the coprecipitation method has become the mainstream synthesis method of layered Ni-based cathode materials due to its advantages of easy control of element proportion, uniform element distribution, regular particle morphology, and suitability for large-scale production. However, a large number of crystal defects, such as grain boundaries and holes, inherited from the precursors which are composed of nano-sized primary particles with random orientations largely weaken the structural stability of the secondary spheres [23]. Thereby, the resulted in intergranular cracks expose the newly generated surface to electrolytes and lead to severe side reactions and oxygen release, especially under thermal failure conditions [119]. Therefore, it is very important to design the inner structure to improve the thermal stability of layered Ni-based cathode materials.

The ordering of primary particles is a new strategy to improve thermal stability in recent years. Interestingly, the introduction of W [52], B [120,121], Ta [122] and Sn [123] into NCM materials can selectively lower the (003) surface energy and result in preferential (003) faceting, thereby leading to the formation of elongated primary particles arranging radially from surface to interior. The radial structure can absorb the anisotropic lattice strain and preserve the mechanical integrity of the cathode particles during cycling. As shown in Figure 7, microcrack suppression protects the particle interior from detrimental electrolyte attack and greatly enhances the thermal stability of Ni-based cathode material.

In addition to the induction by high-valence ion doping, the radially microstructure can also be designed by regulating ammonia concentration to linear change during the co-precipitation process [124].

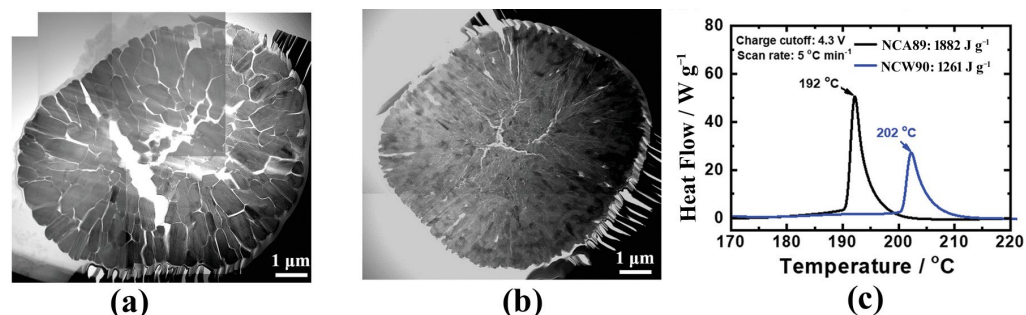


Figure 7. Bright-field STEM mosaic image of a cross-section of (a) NCA89 and (b) NCW90 at charged to 4.3 V, and (c) DSC profiles for NCA89 and NCW90 in the delithiated state at 4.3 V [52].

Single crystallization is another promising approach to strengthen the particle and mitigate the intergranular cracks. Dahn's group has done a lot of work in the single crystal (SC) NCM materials and investigated their synthesis conditions and properties in detail [125–129]. Theoretically, single crystal particles have no grain boundaries, which means the side reactions are limited to the particle surface, but little liquid electrolyte can penetrate in. The single crystal NCM523 was charged and held at 4.4, 4.5, and 4.6 V for 100 h under 40 °C, surprisingly, with no oxygen or other gas generation being detected within detection limits, showing greatly enhanced structural stability [126]. Particularly, crystal gaps inside the polycrystalline (PC) cathode materials will increase the inhomogeneity of PC particles during charging and discharging. The structural damage becomes more serious along with the rise of the delithiation state. The damaged structure can reduce the binding of oxygen and become the initiating factor of oxygen release in advance. As shown in Figure 8, the single crystal NCM622 and NCM811 materials clearly have better thermal stabilities [130]. Other studies also indicate that single-crystal materials have a higher exothermic peak or a reduced heat generation [131–134]. Nevertheless, the large particle size (~4 μm or larger) for single crystals limits the diffusion of lithium ions and scarifies the rate performance especially [135]. In addition, reversible planar gliding and microcracking along the (003) plane in a single-crystalline Ni-rich cathode were also observed during charge-discharge cycles because of the localized stresses induced by a concentration gradient of Li atoms in the lattice [136]. Therefore, it is necessary to further modify the single-crystal Ni-based materials with ion doping and surface engineering to balance the thermal improvement and electrochemical properties.

3.4. Synergistic Effect of Multiple Modifications

According to the current research progress, a single modification technology has improved the thermal stability of the ternary material, but most of the thermal decomposition peak temperatures are only delayed by 10~20 °C, which is not enough to solve the thermal runaway of the battery. Combinations of multiple modifications have attracted more and more attention due to the synergistic effect to improve the performance of cathode materials. Kim et al., synthesized Al-doped NCM622 full gradient material, whose cyclic stability can support more than 10 years of cycle life theoretically [137]. The research of Feng et al. shows that the electrochemical performance of ternary materials can be significantly improved by using doping and coating together [138]. Other studies also show that the synergistic use of single crystallization and doping/coating has better improvement on ternary materials than the single one [139–143]. Therefore, composite modification technology shows excellent synergistic improvement effects and is an important development direction in the field of ternary materials.

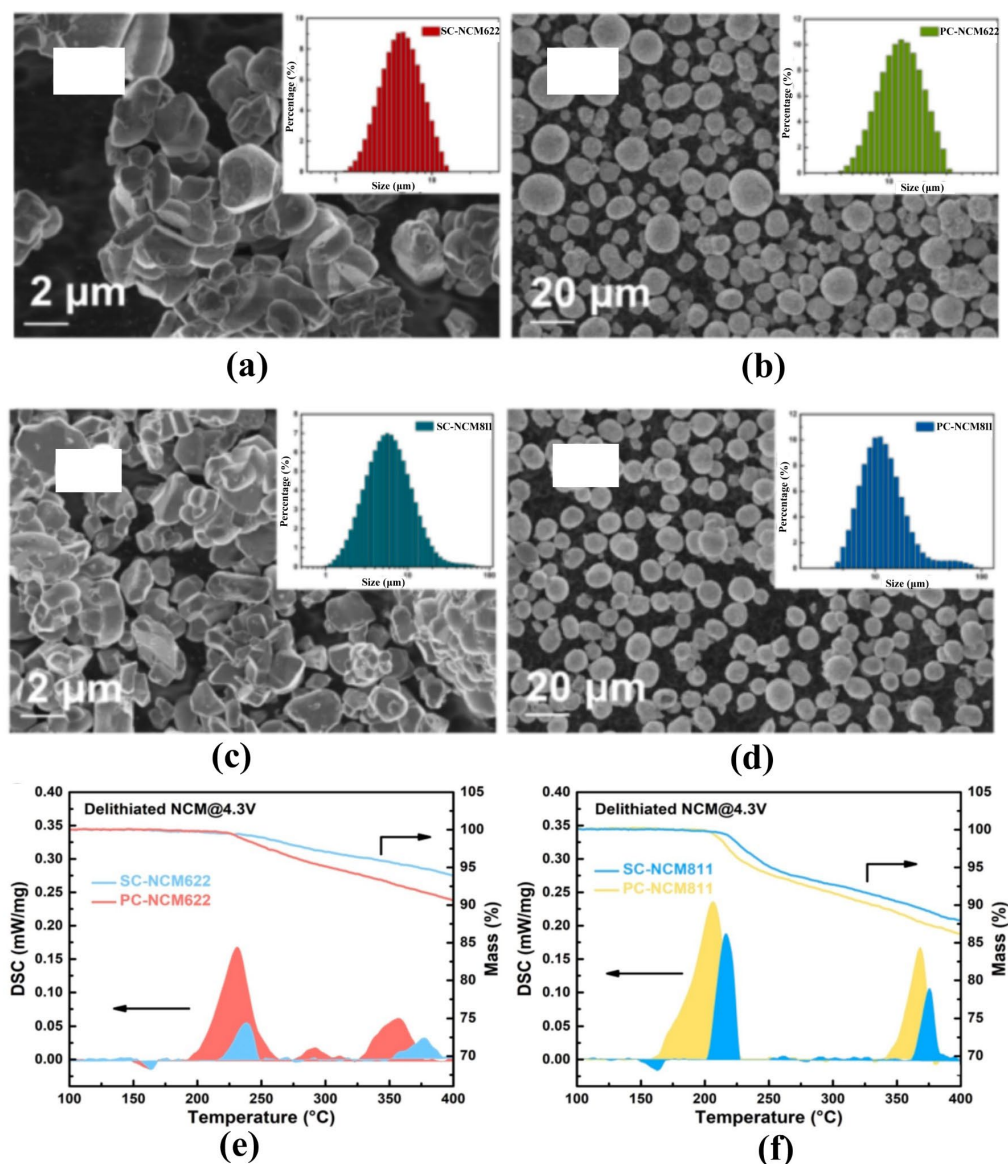


Figure 8. SEM and particle size analyzer test results of (a) SC-NCM622, (b) PC-NCM622, (c) SC-NCM811, (d) PC-NCM811, and TG-DSC test results of the above materials (e) NCM622 and (f) NCM811 [130].

3.5. Other Strategies for LiTMO₂ Battery Safety

A lithium-ion battery is an integration of many materials, and any one of them may affect the safety of the battery. Generally, the liquid electrolyte is the weakest part of a battery because of its flammability, easy decomposability, and chemical instability. Film-forming additives [144–146] and flame retardant additives [147–149] can enhance the thermal stability of liquid electrolytes, thus improving the LiTMO₂ battery safety. Besides, all-solid-state batteries based on solid electrolytes may be expected to solve the thermal runaway of batteries once and for all since there is no combustible liquid electrolyte at all if the challenge of ionic conductivity, and, in particular, interface problems between electrolyte/electrolyte and electrolyte/electrode would be solved [150–152]. Other strategies, such as Al₂O₃-coated separator [153,154], non-flammable fluorinated polyimide binder [155,156], and positive temperature coefficient (PTC) protecting layer [157,158], have also been investigated to improve battery safety from different aspects.

4. Outlook and Conclusions

Despite the high energy density of layered LiTMO_2 materials, the safety issue is still the greatest challenge for large-scale applications although there are already millions of electric vehicles running around the world. The battery safety is strongly affected by the thermal stability of layered Ni-based cathode materials, which attributes to the compositions, oxygen release due to phase transition, and gas evolution. The oxygen release from delithiated layered cathode materials (such as Ni-based materials and Li-rich materials) is the greatest obstacle to improving battery safety, and the mechanism of oxygen evolution needs more detailed research. The corresponding strategies, mainly including elements doping, surface engineering, and microstructure design have been extensively studied and some of the technologies have been successfully applied in industrial productions. The combined use of various modifications can bring synergistic effects to achieve further improvement on the thermal stability of layered Ni-based cathode materials and deserves more explorations. Nevertheless, it makes us feel disappointed and pessimistic that no single technology, at least we have not found it for now, can completely solve the oxygen release problem of layered oxides cathodes.

According to the fire tetrahedron, essentially all four elements, including fuel, heat, oxygen, and a chemical chain reaction, must be present for fire to occur. Removal of any one of these essential elements will result in the fire being extinguished. As illustrated in Figure 9, it is expected to improve the safety of a lithium-ion battery using layered Ni-based materials from the aspects of heat (exothermic), fuel (electrolyte), and chemical reaction chain. Given the fact that most of the combustibles are organic electrolyte, all solid-state batteries based on solid electrolyte may be expected to solve the thermal runaway of batteries once and for all. The PTC inside a cell and combustion blocking layer (asbestos, for example) in a battery pack can effectively cut off the reaction chain. While the heat generation inside a battery is more complicated. We found that almost all cathode materials have a sharp exothermic peak, which corresponds to the sharp temperature rise of T_2 inside the battery. Thus, it is possible to split the sharp peak into two or more small peaks by the above modifications in order to slow down the heat accumulation inside a battery. From a macroscopic perspective, it is a systematic engineering to solve the problem of thermal runaway of the battery from the aspects of materials, cell, battery-package structure design and system integration.

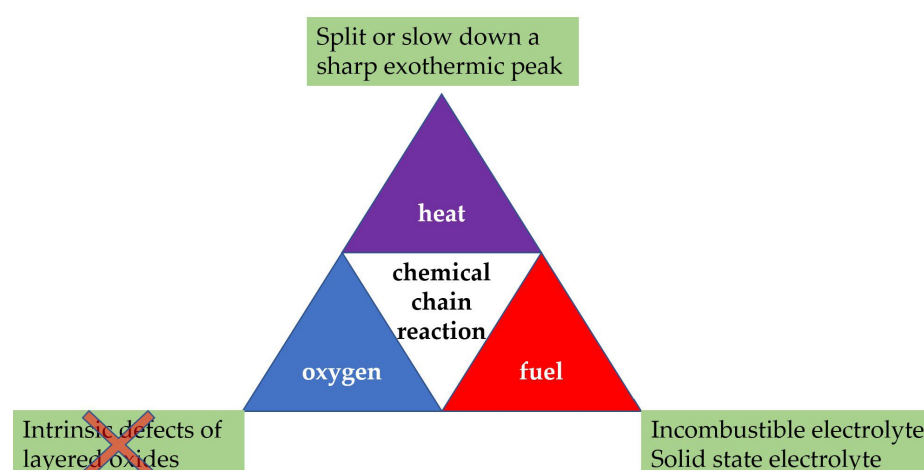


Figure 9. Scheme of the fire tetrahedron and possible corresponding strategies to improve battery safety.

Author Contributions: Conceptualization, Z.T., D.F., Y.X., L.C., X.Z. and Q.M.; methodology, D.F. and Y.X.; validation, Y.X., L.C. and Q.M.; investigation, Z.T., D.F., L.C., X.Z. and Q.M.; resources, Y.X. and X.Z.; data curation, Z.T., D.F. and X.Z.; writing—original draft preparation, Z.T. and D.F.; writing—review and editing, Z.T., D.F., Q.M. and L.C.; supervision, Z.T. and L.C.; funding acquisition, D.F. All authors have read and agreed to the published version of the manuscript.

Funding: This research was funded by the Key Scientific Research Projects of Universities in Henan province (20B150027); and the Project of Fundamental Researches and Applied Fundamental Researches of Zhengzhou Science and Technology Bureau (zkk202107).

Conflicts of Interest: The authors declare no conflict of interest.

References

1. Viswanathan, V.; Epstein, A.H.; Chiang, Y.-M.; Takeuchi, E.; Bradley, M.; Langford, J.; Winter, M. The Challenges and Opportunities of Battery-Powered Flight. *Nature* **2022**, *601*, 519–525. [[CrossRef](#)] [[PubMed](#)]
2. Lai, X.; Yao, J.; Jin, C.Y.; Feng, X.N.; Wang, H.B.; Xu, C.S.; Zheng, Y.J. A Review of Lithium-Ion Battery Failure Hazards: Test Standards, Accident Analysis, and Safety Suggestions. *Batteries* **2022**, *8*, 248–275. [[CrossRef](#)]
3. Li, M.; Lu, J.; Chen, Z.; Amine, K. 30 Years of Lithium-Ion Batteries. *Adv. Mater.* **2018**, *30*, 1800561. [[CrossRef](#)]
4. Xie, J.; Lu, Y.C. A Retrospective on Lithium-Ion Batteries. *Nat. Commun.* **2020**, *11*, 2499. [[CrossRef](#)]
5. Jung, W.W.; Jeong, J.; Kim, J.; Chang, D. Optimization of Hybrid Off-Grid System Consisting of Renewables and Li-Ion Batteries. *J. Power Sources* **2020**, *451*, 227754. [[CrossRef](#)]
6. Wentker, M.; Greenwood, M.; Leker, J. A Bottom-Up Approach to Lithium-Ion Battery Cost Modeling with a Focus on Cathode Active Materials. *Energies* **2019**, *12*, 504. [[CrossRef](#)]
7. Julien, C.M.; Mauger, A. NCA, NCM811, and the Route to Ni-rich Lithium-Ion Batteries. *Energies* **2020**, *13*, 6363. [[CrossRef](#)]
8. Hu, G.; Huang, P.; Bai, Z.; Wang, Q.; Qi, K. Comprehensively Analysis the Failure Evolution and Safety Evaluation of Automotive Lithium Ion Battery. *ETransportation* **2021**, *10*, 100140. [[CrossRef](#)]
9. Sun, P.; Bisschop, R.; Niu, H.; Huang, X. A Review of Battery Fires in Electric Vehicles. *Fire Technol.* **2020**, *56*, 1361–1410. [[CrossRef](#)]
10. Zhang, Z.; Ding, T.; Zhou, Q.; Sun, Y.; Qu, M.; Zeng, Z.; Ju, Y.; Li, L.; Wang, K.; Chi, F. A Review of Technologies and Applications on Versatile Energy Storage Systems. *Renew. Sustain. Energy Rev.* **2021**, *148*, 111263. [[CrossRef](#)]
11. Chombo, P.V.; Laounual, Y. A Review of Safety Strategies of a Li-Ion Battery. *J. Power Sources* **2020**, *478*, 228649. [[CrossRef](#)]
12. Feng, X.N.; Ren, D.; He, X.; Ouyang, M.G. Mitigating Thermal Runaway of Lithium-Ion Batteries. *Joule* **2020**, *4*, 743–770. [[CrossRef](#)]
13. Feng, X.N.; Zheng, S.Q.; He, X.M.; Wang, L.; Wang, Y.; Ren, D.S.; Ouyang, M.G. Time Sequence Map for Interpreting the Thermal Runaway Mechanism of Lithium-Ion Batteries with $\text{LiNi}_x\text{Co}_y\text{Mn}_z\text{O}_2$ Cathode. *Front. Energy Res.* **2018**, *6*, 126. [[CrossRef](#)]
14. Chen, Y.Q.; Kang, Y.Q.; Zhao, Y.; Wang, L.; Liu, J.L.; Li, Y.X.; Liang, Z.; He, X.M.; Li, X.; Tavajohi, N.; et al. A Review of Lithium-Ion Battery Safety Concerns: The Issues, Strategies, and Testing Standards. *J. Energy Chem.* **2021**, *59*, 83–99. [[CrossRef](#)]
15. Liang, C.; Jiang, L.H.; Wei, Z.S.; Zhang, W.H.; Wang, Q.S.; Sun, J.H. Insight into the Structural Evolution and Thermal Behavior of $\text{LiNi}_{0.8}\text{Co}_{0.1}\text{Mn}_{0.1}\text{O}_2$ Cathode Under Deep Charge. *J. Energy Chem.* **2022**, *65*, 424–432. [[CrossRef](#)]
16. Yang, M.J.; Ye, Y.J.; Yang, A.J.; Jiang, Z.Y.; Wang, X.H.; Yuan, H.; Rong, M.Z. Comparative Study on Aging and Thermal Runaway of Commercial LiFePO_4 /Graphite Battery undergoing Slight Overcharge Cycling. *J. Energy Chem.* **2022**, *50*, 104691. [[CrossRef](#)]
17. Zhou, Z.Z.; Zhou, X.D.; Cao, B.; Yang, L.Z.; Liew, K.M. Investigating the Relationship between Heating Temperature and Thermal Runaway of Prismatic Lithium-Ion Battery with LiFePO_4 as Cathode. *Energy* **2022**, *256*, 124714. [[CrossRef](#)]
18. Wang, Z.P.; Yuan, J.; Zhu, X.Q.; Wang, H.; Huang, L.; Wang, Y.T.; Xu, S.Q. Overcharge-to-Thermal-Runaway Behavior and Safety Assessment of Commercial Lithium-Ion Cells with Different Cathode Materials: A Comparison Study. *J. Energy Chem.* **2021**, *55*, 484–498. [[CrossRef](#)]
19. Feng, X.N.; Zheng, S.Q.; Ren, D.S.; He, X.M.; Wang, L.; Liu, X.; Li, M.G.; Ouyang, M.G. Key Characteristics for Thermal Runaway of Li-Ion Batteries. *Energy Procedia* **2019**, *158*, 4684–4689. [[CrossRef](#)]
20. Lyu, Y.C.; Wu, X.; Wang, K.; Feng, Z.J.; Cheng, T.; Liu, Y.; Wang, M.; Chen, R.M.; Xu, L.M.; Zhou, J.J.; et al. An Overview on the Advances of LiCoO_2 Cathodes for Lithium-Ion Batteries. *Adv. Energy Mater.* **2021**, *11*, 2000982. [[CrossRef](#)]
21. Zhang, J.N.; Li, Q.H.; Ouyang, C.; Yu, X.; Ge, M.; Huang, X.J.; Hu, E.; Ma, C.; Li, S.F.; Xiao, R.; et al. Trace Doping of Multiple Elements Enables Stable Battery Cycling of LiCoO_2 at 4.6 V. *Nat. Energy* **2019**, *4*, 594–603. [[CrossRef](#)]
22. Bianchini, M.; Roca-Ayats, M.; Hartmann, P.; Brezesinski, T.; Janek, J. There and Back Again—the Journey of LiNiO_2 as a Cathode Active Material. *Angew. Chem. Int. Ed.* **2019**, *58*, 10434–10458. [[CrossRef](#)] [[PubMed](#)]
23. Tang, Z.F.; Bao, J.J.; Du, Q.X.; Shao, Y.; Gao, M.H.; Zou, B.K.; Chen, C.H. Surface Surgery of the Nickel-Rich Cathode Material $\text{LiNi}_{0.815}\text{Co}_{0.15}\text{Al}_{0.035}\text{O}_2$: Toward a Complete and Ordered Surface Layered Structure and Better Electrochemical Properties. *ACS Appl. Mater. Interfaces* **2016**, *8*, 34879–34887. [[CrossRef](#)] [[PubMed](#)]
24. Liu, Z.L.; Yu, A.S.; Lee, J.Y. Synthesis and Characterization of $\text{LiNi}_{1-x-y}\text{Co}_x\text{Mn}_y\text{O}_2$ as the Cathode Materials of Secondary Lithium Batteries. *J. Power Sources* **1999**, *81*, 416–419. [[CrossRef](#)]

25. Wang, B.; Zhang, F.L.; Zhou, X.A.; Wang, P.; Wang, J.; Ding, H.; Dong, H.; Liang, W.B.; Zhang, N.S.; Li, S.Y. Which of the Nickel-Rich NCM and NCA is Structurally Superior as a Cathode Material for Lithium-Ion Batteries? *J. Mater. Chem. A* **2021**, *9*, 13540–13551. [[CrossRef](#)]
26. Kim, U.H.; Kuo, L.Y.; Kaghazchi, P.; Yoon, C.S.; Sun, Y.K. Quaternary Layered Ni-Rich NCMA Cathode for Lithium-Ion Batteries. *ACS Energy Lett.* **2019**, *4*, 576–582. [[CrossRef](#)]
27. Noh, H.J.; Youn, S.; Yoon, C.S.; Sun, Y.K. Comparison of the Structural and Electrochemical Properties of Layered $\text{Li}[\text{Ni}_x\text{Co}_y\text{Mn}_z]\text{O}_2$ ($x = 1/3, 0.5, 0.6, 0.7, 0.8$ and 0.85) Cathode Material for Lithium-Ion Batteries. *J. Power Sources* **2013**, *233*, 121–130. [[CrossRef](#)]
28. Bak, S.M.; Hu, E.; Zhou, Y.; Yu, X.; Senanayake, S.D.; Cho, S.J.; Kim, K.B.; Chung, K.Y.; Yang, X.Q.; Nam, K.W. Structural Changes and Thermal Stability of Charged $\text{LiNi}_x\text{Mn}_y\text{Co}_z\text{O}_2$ Cathode Materials Studied by Combined In Situ Time-Resolved XRD and Mass Spectroscopy. *ACS Appl. Mater. Interfaces* **2014**, *6*, 22594–22601. [[CrossRef](#)]
29. Dixit, M.; Markovsky, B.; Schipper, F.; Aurbach, D.; Major, D.T. Origin of Structural Degradation during Cycling and Low Thermal Stability of Ni-Rich Layered Transition Metal-Based Electrode Materials. *J. Phys. Chem. C* **2017**, *121*, 22628–22636. [[CrossRef](#)]
30. Tuccillo, M.; Palumbo, O.; Pavone, M.; Muñoz-García, A.B.; Paolone, A.; Brutti, S. Analysis of the Phase Stability of LiMO_2 Layered Oxides ($M = \text{Co}, \text{Mn}, \text{Ni}$). *Crystals* **2020**, *10*, 526. [[CrossRef](#)]
31. Duan, Y.; Yang, L.; Zhang, M.J.; Chen, Z.; Bai, J.; Amine, K.; Pan, F.; Wang, F. Insights into Li/Ni Ordering and Surface Reconstruction During Synthesis of Ni-Rich Layered Oxides. *J. Mater. Chem. A* **2019**, *7*, 513–519. [[CrossRef](#)]
32. Liang, C.; Kong, F.; Longo, R.C.; Kc, S.; Kim, J.S.; Jeon, S.; Choi, S.; Cho, K. Unraveling the Origin of Instability in Ni-Rich $\text{LiNi}_{1-2x}\text{Co}_x\text{Mn}_x\text{O}_2$ (NCM) Cathode Materials. *J. Phys. Chem. C* **2016**, *120*, 6383–6393. [[CrossRef](#)]
33. Jamil, S.; Wang, G.; Yang, L.; Xie, X.; Cao, S.; Liu, H.; Chang, B.B.; Wang, X. Suppressing H2–H3 Phase Transition in High Ni–Low Co Layered Oxide Cathode Material by Dual Modification. *J. Mater. Chem. A* **2020**, *8*, 21306–21316. [[CrossRef](#)]
34. Kuo, L.Y.; Guillon, O.; Kaghazchi, P. Origin of Structural Phase Transitions in Ni-Rich $\text{Li}_x\text{Ni}_{0.8}\text{Co}_{0.1}\text{Mn}_{0.1}\text{O}_2$ with Lithiation/Delithiation: A First-Principles Study. *ACS Sustain. Chem. Eng.* **2021**, *9*, 7437–7446. [[CrossRef](#)]
35. Wang, C.; Han, L.; Zhang, R.; Cheng, H.; Mu, L.; Kisslinger, K.; Zou, P.; Ren, Y.; Cao, P.; Lin, F.; et al. Resolving Atomic-Scale Phase Transformation and Oxygen Loss Mechanism in Ultrahigh-Nickel Layered Cathodes for Cobalt-Free Lithium-Ion Batteries. *Matter* **2021**, *4*, 2013–2026. [[CrossRef](#)]
36. Bak, S.M.; Nam, K.W.; Chang, W.; Yu, X.; Hu, E.; Hwang, S.; Stach, E.A.; Kim, K.B.; Yang, X.Q. Correlating Structural Changes and Gas Evolution during the Thermal Decomposition of Charged $\text{Li}_x\text{Ni}_{0.8}\text{Co}_{0.15}\text{Al}_{0.05}\text{O}_2$ Cathode Materials. *Chem. Mater.* **2013**, *25*, 337–351. [[CrossRef](#)]
37. Ryu, H.H.; Park, K.J.; Yoon, C.S.; Sun, Y.K. Capacity Fading of Ni-Rich $\text{Li}[\text{Ni}_x\text{Co}_y\text{Mn}_{1-x-y}]\text{O}_2$ ($0.6 \leq x \leq 0.95$) Cathodes for High-Energy-Density Lithium-Ion Batteries: Bulk or Surface Degradation? *Chem. Mater.* **2018**, *30*, 1155–1163. [[CrossRef](#)]
38. Yin, S.; Deng, W.; Chen, J.; Gao, X.; Zou, G.; Hou, H.; Ji, X. Fundamental and Solutions of Microcrack in Ni-Rich Layered Oxide Cathode Materials of Lithium-Ion Batteries. *Nano Energy* **2021**, *83*, 105854. [[CrossRef](#)]
39. Yan, P.; Zheng, J.; Gu, M.; Xiao, J.; Zhang, J.G.; Wang, C.M. Intragranular Cracking as a Critical Barrier for High-Voltage Usage of Layer-Structured Cathode for Lithium-Ion Batteries. *Nat. Commun.* **2017**, *8*, 1–9. [[CrossRef](#)]
40. Besli, M.M.; Xia, S.; Kuppan, S.; Huang, Y.; Metzger, M.; Shukla, A.K.; Schneider, G.; Hellstrom, S.; Christensen, J.; Doeff, M.M.; et al. Mesoscale Chemomechanical Interplay of the $\text{LiNi}_{0.8}\text{Co}_{0.15}\text{Al}_{0.05}\text{O}_2$ Cathode in Solid-State Polymer Batteries. *Chem. Mater.* **2019**, *31*, 491–501. [[CrossRef](#)]
41. Liu, T.; Yu, L.; Liu, J.; Lu, J.; Bi, X.; Dai, A.; Li, M.; Li, M.F.; Hu, Z.; Ma, L.; et al. Understanding Co Roles towards Developing Co-Free Ni-Rich Cathodes for Rechargeable Batteries. *Nat. Energy* **2021**, *6*, 277–286. [[CrossRef](#)]
42. Kim, Y. Encapsulation of $\text{LiNi}_{0.5}\text{Co}_{0.2}\text{Mn}_{0.3}\text{O}_2$ with a Thin Inorganic Electrolyte Film to Reduce Gas Evolution in the Application of Lithium Ion Batteries. *Phys. Chem. Chem. Phys.* **2013**, *15*, 6400–6405. [[CrossRef](#)] [[PubMed](#)]
43. Cheng, F.; Zhang, X.; Wei, P.; Sun, S.; Xu, Y.; Li, Q.; Fang, C.; Han, J.; Huang, Y. Tailoring Electrolyte Enables High-Voltage Ni-rich NCM Cathode Against Aggressive Cathode Chemistries for Li-Ion Batteries. *Sci. Bull.* **2022**, *67*, 2225–2234. [[CrossRef](#)] [[PubMed](#)]
44. Renfrew, S.E.; McCloskey, B.D. Residual Lithium Carbonate Predominantly Accounts for First Cycle CO_2 and CO Outgassing of Li-Stoichiometric and Li-Rich Layered Transition-Metal Oxides. *J. Am. Chem. Soc.* **2017**, *139*, 17853–17860. [[CrossRef](#)]
45. Kim, Y.; Park, H.; Warner, J.H.; Manthiram, A. Unraveling the Intricacies of Residual Lithium in High-Ni Cathodes for Lithium-Ion Batteries. *ACS Energy Lett.* **2021**, *6*, 941–948. [[CrossRef](#)]
46. Wachs, S.J.; Behling, C.; Ranninger, J.; Möller, J.; Mayrhofer, K.J.; Berkes, B.B. Online Monitoring of Transition-Metal Dissolution from a High-Ni-Content Cathode Material. *ACS Appl. Mater. Interfaces* **2021**, *13*, 33075–33082. [[CrossRef](#)]
47. Li, W. An Unpredictable Hazard in Lithium-Ion Batteries from Transition Metal Ions: Dissolution from Cathodes, Deposition on Anodes and Elimination Strategies. *J. Electrochem. Soc.* **2020**, *167*, 90514. [[CrossRef](#)]
48. Jeong, M.; Kim, H.; Lee, W.; Ahn, S.J.; Lee, E.; Yoon, W.S. Stabilizing Effects of Al-Doping on Ni-Rich $\text{LiNi}_{0.80}\text{Co}_{0.15}\text{Mn}_{0.05}\text{O}_2$ Cathode for Li Rechargeable Batteries. *J. Power Sources* **2020**, *474*, 228592. [[CrossRef](#)]
49. Levartovsky, Y.; Wu, X.; Erk, C.; Maiti, S.; Grinblat, J.; Talianker, M.; Aurbach, D. Enhancement of Structural, Electrochemical, and Thermal Properties of Ni-Rich $\text{LiNi}_{0.85}\text{Co}_{0.1}\text{Mn}_{0.05}\text{O}_2$ Cathode Materials for Li-Ion Batteries by Al and Ti Doping. *Batter. Supercaps* **2021**, *4*, 221–231. [[CrossRef](#)]

50. Zhang, H.; Wu, K.; Li, N.; Deng, X.; Jiao, J.; Zhao, E.; Yin, W.; Wang, B.; Zhao, J.; Xiao, X. Enhancing Thermal and High-Voltage Cycling Stability of Ni-Rich Layered Cathodes through a Ti-Doping-Induced Surface-Disordered Structure. *ACS Appl. Energy Mater.* **2022**, *5*, 12673–12681. [[CrossRef](#)]
51. Lipson, A.L.; Durham, J.L.; LeResche, M.; Abu-Baker, I.; Murphy, M.J.; Fister, T.T.; Wang, L.; Zhou, F.; Liu, L.; Kim, K.; et al. Improving the Thermal Stability of NMC 622 Li-Ion Battery Cathodes through Doping during Coprecipitation. *ACS Appl. Mater. Interfaces* **2020**, *12*, 18512–18518. [[CrossRef](#)] [[PubMed](#)]
52. Ryu, H.H.; Park, K.J.; Yoon, D.R.; Aishova, A.; Yoon, C.S.; Sun, Y.K. Li[Ni_{0.9}Co_{0.09}W_{0.01}]O₂: A New Type of Layered Oxide Cathode with High Cycling Stability. *Adv. Energy Mater.* **2019**, *9*, 1902698. [[CrossRef](#)]
53. Kim, U.H.; Jun, D.W.; Park, K.J.; Zhang, Q.; Kaghazchi, P.; Aurbach, D.; Major, D.T.; Goobes, G.; Dixit, M.; Leifer, N.; et al. Pushing the Limit of Layered Transition Metal Oxide Cathodes for High-Energy Density Rechargeable Li Ion Batteries. *Energy Environ. Sci.* **2018**, *11*, 1271–1279. [[CrossRef](#)]
54. Sim, S.J.; Lee, S.H.; Jin, B.S.; Kim, H.S. Improving the Electrochemical Performances using a V-Doped Ni-Rich NCM Cathode. *Sci. Rep.* **2019**, *9*, 8952. [[CrossRef](#)] [[PubMed](#)]
55. Susai, F.A.; Kovacheva, D.; Chakraborty, A.; Kravchuk, T.; Ravikumar, R.; Talianker, M.; Grinblat, J.; Burstein, L.; Kauffmann, Y.; Major, D.T.; et al. Improving Performance of LiNi_{0.8}Co_{0.1}Mn_{0.1}O₂ Cathode Materials for Lithium-Ion Batteries by Doping with Molybdenum-Ions: Theoretical and Experimental Studies. *ACS Appl. Energy Mater.* **2019**, *2*, 4521–4534. [[CrossRef](#)]
56. Chen, Y.H.; Zhang, J.; Li, Y.; Zhang, Y.F.; Huang, S.P.; Lin, W.; Chen, W.K. Effects of Doping High-Valence Transition Metal (V, Nb and Zr) Ions on the Structure and Electrochemical Performance of LIB Cathode Material LiNi_{0.8}Co_{0.1}Mn_{0.1}O₂. *Phys. Chem. Chem. Phys.* **2021**, *23*, 11528–11537. [[CrossRef](#)] [[PubMed](#)]
57. Min, K.; Seo, S.W.; Song, Y.Y.; Lee, H.S.; Cho, E. A First-Principles Study of the Preventive Effects of Al and Mg Doping on the Degradation in LiNi_{0.8}Co_{0.1}Mn_{0.1}O₂ Cathode Materials. *Phys. Chem. Chem. Phys.* **2017**, *19*, 1762–1769. [[CrossRef](#)] [[PubMed](#)]
58. Shen, Y.; Yao, X.; Zhang, J.; Wang, S.; Zhang, D.; Yin, D.; Wang, L.; Zhang, Y.; Hu, J.; Cheng, Y.; et al. Sodium Doping Derived Electromagnetic Center of Lithium Layered Oxide Cathode Materials with Enhanced Lithium Storage. *Nano Energy* **2022**, *94*, 106900. [[CrossRef](#)]
59. Feng, L.; Liu, Y.; Wu, L.; Qin, W.; Yang, Z. Enhancement on Inter-Layer Stability on Na-Doped LiNi_{0.6}Co_{0.2}Mn_{0.2}O₂ Cathode Material. *Powder Technol.* **2021**, *388*, 166–175. [[CrossRef](#)]
60. Wang, Y.Y.; Sun, Y.Y.; Liu, S.; Li, G.R.; Gao, X.P. Na-doped LiNi_{0.8}Co_{0.15}Al_{0.05}O₂ with Excellent Stability of Both Capacity and Potential as Cathode Materials for Li-Ion Batteries. *ACS Appl. Energy Mater.* **2018**, *1*, 3881–3889. [[CrossRef](#)]
61. Xie, H.; Du, K.; Hu, G.; Peng, Z.; Cao, Y. The Role of Sodium in LiNi_{0.8}Co_{0.15}Al_{0.05}O₂ Cathode Material and its Electrochemical Behaviors. *J. Phys. Chem. C* **2016**, *120*, 3235–3241. [[CrossRef](#)]
62. Li, C.F.; Chen, L.D.; Wu, L.; Liu, Y.; Hu, Z.Y.; Cui, W.J.; Dong, W.D.; Liu, X.; Yu, W.B.; Li, Y.; et al. Directly Revealing the Structure-Property Correlation in Na⁺-Doped Cathode Materials. *Appl. Surf. Sci.* **2023**, *612*, 155810. [[CrossRef](#)]
63. Gomez-Martin, A.; Reissig, F.; Frankenstein, L.; Heidbüchel, M.; Winter, M.; Placke, T.; Schmich, R. Magnesium Substitution in Ni-Rich NMC Layered Cathodes for High-Energy Lithium Ion Batteries. *Adv. Energy Mater.* **2022**, *12*, 2103045. [[CrossRef](#)]
64. Liu, X.; Wang, S.; Wang, L.; Wang, K.; Wu, X.; Zhou, P.; Miao, Z.; Zhou, J.; Zhao, Y.; Zhuo, S. Stabilizing the High-Voltage Cycle Performance of LiNi_{0.8}Co_{0.1}Mn_{0.1}O₂ Cathode Material by Mg Doping. *J. Power Sources* **2019**, *438*, 227017. [[CrossRef](#)]
65. Song, J.H.; Kapyrou, A.; Choi, H.S.; Yu, B.Y.; Matulevich, E.; Kang, S.H. Suppression of Irreversible Capacity Loss in Li-Rich Layered Oxide by Fluorine Doping. *J. Power Sources* **2016**, *313*, 65–72. [[CrossRef](#)]
66. Shin, H.S.; Park, S.H.; Yoon, C.S.; Sun, Y.K. Effect of Fluorine on the Electrochemical Properties of Layered Li[Ni_{0.43}Co_{0.22}Mn_{0.35}]O₂ Cathode Materials via a Carbonate Process. *Electrochim. Solid-State Lett.* **2005**, *8*, A559. [[CrossRef](#)]
67. Kim, H.; Kim, S.B.; Park, D.H.; Park, K.W. Fluorine-Doped LiNi_{0.8}Mn_{0.1}Co_{0.1}O₂ Cathode for High-Performance Lithium-Ion Batteries. *Energies* **2020**, *13*, 4808. [[CrossRef](#)]
68. Woo, S.U.; Park, B.C.; Yoon, C.S.; Myung, S.T.; Prakash, J.; Sun, Y.K. Improvement of Electrochemical Performances of Li[Ni_{0.8}Co_{0.1}Mn_{0.1}]O₂ Cathode Materials by Fluorine Substitution. *J. Electrochem. Soc.* **2007**, *154*, A649. [[CrossRef](#)]
69. Zhou, S.; Wang, G.; Tang, W.; Xiao, Y.; Yan, K. Enhanced Rate Performance and High Potential as well as Decreased Strain of LiNi_{0.6}Co_{0.2}Mn_{0.2}O₂ by Facile Fluorine Modification. *Electrochim. Acta* **2018**, *261*, 565–577. [[CrossRef](#)]
70. Binder, J.O.; Culver, S.P.; Pinedo, R.; Weber, D.A.; Friedrich, M.S.; Gries, K.I.; Volz, K.; Zeier, W.G.; Janek, J. Investigation of Fluorine and Nitrogen as Anionic Dopants in Nickel-Rich Cathode Materials for Lithium-Ion Batteries. *ACS Appl. Mater. Interfaces* **2018**, *10*, 44452–44462. [[CrossRef](#)]
71. Liu, K.; Zhang, Q.; Dai, S.; Li, W.; Liu, X.; Ding, F.; Zhang, J. Synergistic Effect of F-Doping and LiF Coating on Improving the High-Voltage Cycling Stability and Rate Capacity of LiNi_{0.5}Co_{0.2}Mn_{0.3}O₂ Cathode Materials for Lithium-Ion Batteries. *ACS Appl. Mater. Interfaces* **2018**, *10*, 34153–34162. [[CrossRef](#)] [[PubMed](#)]
72. Breddemann, U.; Krossing, I. Review on Synthesis, Characterization, and Electrochemical Properties of Fluorinated Nickel-Cobalt-Manganese Cathode Active Materials for Lithium-Ion Batteries. *ChemElectroChem* **2020**, *7*, 1389–1430. [[CrossRef](#)]
73. Si, Z.; Shi, B.; Huang, J.; Yu, Y.; Han, Y.; Zhang, J.; Li, W. Titanium and Fluorine Synergetic Modification Improves the Electrochemical Performance of Li(Ni_{0.8}Co_{0.1}Mn_{0.1})O₂. *J. Mater. Chem. A* **2021**, *9*, 9354–9363. [[CrossRef](#)]
74. Zhu, F.; Shi, Y.; Hu, G.; Peng, Z.; Cao, Y.; Sun, Q.; Xue, Z.; Zhang, Y.; Du, K. Enhanced electrochemical performance of LiNi_{0.8}Co_{0.1}Mn_{0.1}O₂ via titanium and boron co-doping. *Ceram. Int.* **2021**, *47*, 3070–3078. [[CrossRef](#)]

75. Wang, J.; Nie, Y.; Miao, C.; Tan, Y.; Wen, M.; Xiao, W. Enhanced Electrochemical Properties of Ni-Rich Layered Cathode Materials via Mg^{2+} and Ti^{4+} Co-Doping for Lithium-Ion Batteries. *J. Colloid Interface Sci.* **2021**, *601*, 853–862. [[CrossRef](#)] [[PubMed](#)]
76. Sun, Y.; Hai, C.; Shen, Y.; Zeng, J.; Zhang, L.; Li, X.; Ren, X.; Dong, S.; Zhang, G.; Sun, C.; et al. Improved Lithium Ion Diffusion and Stability of a $LiNi_{0.8}Co_{0.1}Mn_{0.1}O_2$ Cathode via the Synergistic Effect of Na and Mg Dual-Metal Cations for Lithium Ion Battery. *J. Electrochem. Soc.* **2020**, *167*, 020522.
77. Jamil, S.; Yousaf, A.B.; Yoon, S.H.; Han, D.S.; Yang, L.; Kasak, P.; Wang, X. Dual Cationic Modified High Ni-Low Co Layered Oxide Cathode with a Heteroepitaxial Interface for High Energy-Density Lithium-Ion Batteries. *Chem. Eng. J.* **2021**, *416*, 129118. [[CrossRef](#)]
78. Luo, Z.; Hu, G.; Wang, W.; Peng, Z.; Fang, Z.; Cao, Y.; Huang, J.; Du, K. Enhancing Structural Stability and Electrochemical Properties of Co-Less Ni-Rich Layer Cathode Materials by Fluorine and Niobium Co-Doping. *ACS Appl. Energy Mater.* **2022**, *5*, 10927–10939. [[CrossRef](#)]
79. Chen, Z.; Gong, X.; Zhu, H.; Cao, K.; Liu, Q.; Liu, J.; Li, L.; Duan, J. High performance and structural stability of K and Cl co-doped $LiNi_{0.5}Co_{0.2}Mn_{0.3}O_2$ cathode materials in 4.6 voltage. *Front. Chem.* **2019**, *6*, 643. [[CrossRef](#)] [[PubMed](#)]
80. Yan, J.; Huang, H.; Tong, J.; Li, W.; Liu, X.; Zhang, H.; Huang, H.; Zhou, W. Recent Progress on the Modification of High Nickel Content NCM: Coating, Doping, and Single Crystallization. *Interdiscip. Mater.* **2022**, *1*, 330–353. [[CrossRef](#)]
81. Cao, Z.; Li, Y.; Shi, M.; Zhu, G.; Zhang, R.; Li, X.; Yue, H.; Yang, S. Improvement of the Cycling Performance and Thermal Stability of Lithium-Ion Batteries by Coating Cathode Materials with Al_2O_3 Nano Layer. *J. Electrochem. Soc.* **2017**, *164*, A475. [[CrossRef](#)]
82. Lee, Y.S.; Shin, W.K.; Kannan, A.G.; Koo, S.M.; Kim, D.W. Improvement of the Cycling Performance and Thermal Stability of Lithium-Ion Cells by Double-Layer Coating of Cathode Materials with Al_2O_3 Nanoparticles and Conductive Polymer. *ACS Appl. Mater. Interfaces* **2015**, *7*, 13944–13951. [[CrossRef](#)] [[PubMed](#)]
83. Shi, Y.; Zhang, M.; Qian, D.; Meng, Y.S. Ultrathin Al_2O_3 Coatings for Improved Cycling Performance and Thermal Stability of $LiNi_{0.5}Co_{0.2}Mn_{0.3}O_2$ Cathode Material. *Electrochim. Acta* **2016**, *203*, 154–161. [[CrossRef](#)]
84. Wang, L.; Su, Q.; Shi, W.; Wang, C.; Li, H.; Wang, Y.; Du, G.; Zhang, M.; Zhao, W.; Ding, S.; et al. Optimized Structure Stability and Cycling Performance of $LiNi_{0.8}Co_{0.1}Mn_{0.1}O_2$ through homogeneous nano-thickness Al_2O_3 coating. *Electrochim. Acta* **2022**, *435*, 141411. [[CrossRef](#)]
85. Fan, Q.; Lin, K.; Yang, S.; Guan, S.; Chen, J.; Feng, S.; Liu, J.; Liu, L.; Li, J.; Shi, Z. Constructing Effective TiO_2 Nano-Coating for High-Voltage Ni-Rich Cathode Materials for Lithium Ion Batteries by Precise Kinetic Control. *J. Power Sources* **2020**, *477*, 228745. [[CrossRef](#)]
86. Li, Y.; Liu, X.; Ren, D.; Hsu, H.; Xu, G.L.; Hou, J.; Wang, L.; Feng, X.; Lu, L.; Xu, W.; et al. Toward a High-Voltage Fast-Charging Pouch Cell with TiO_2 Cathode Coating and Enhanced Battery Safety. *Nano Energy* **2020**, *71*, 104643. [[CrossRef](#)]
87. Wang, W.; Wu, L.; Li, Z.; Huang, K.; Jiang, J.; Chen, Z.; Qi, X.; Dou, H.; Zhang, X. In Situ Tuning Residual Lithium Compounds and Constructing TiO_2 Coating for Surface Modification of a Nickel-Rich Cathode toward High-Energy Lithium-Ion Batteries. *ACS Appl. Energy Mater.* **2020**, *3*, 12423–12432. [[CrossRef](#)]
88. Hwang, D.Y.; Sim, S.J.; Jin, B.S.; Kim, H.S.; Lee, S.H. Suppressed microcracking and F penetration of ni-rich layered cathode via the combined effects of titanium dioxide doping and coating. *ACS Appl. Energy Mater.* **2021**, *4*, 1743–1751. [[CrossRef](#)]
89. Khalili Azar, M.; Razmjoo Kholari, M.A.; Esmaeili, M.; Heidari, E.; Hosseini-Hosseinabad, S.M.; Siavash Moakhar, R.; Dolati, A.; Ramakrishna, S. Enhanced Electrochemical Performance and Thermal Stability of ZrO_2 - and rGO - ZrO_2 -Coated $Li[Ni_{0.8}Co_{0.1}Mn_{0.1}]O_2$ Cathode Material for Li-Ion Batteries. *ACS Appl. Energy Mater.* **2020**, *4*, 934–945. [[CrossRef](#)]
90. Ma, F.; Wu, Y.; Wei, G.; Qiu, S.; Qu, J. Enhanced Electrochemical Performance of $LiNi_{0.8}Co_{0.1}Mn_{0.1}O_2$ Cathode via Wet-Chemical Coating of MgO . *J. Solid State Electrochem.* **2019**, *23*, 2213–2224. [[CrossRef](#)]
91. Sharifi-Asl, S.; Lu, J.; Amine, K.; Shahbazian-Yassar, R. Oxygen Release Degradation in Li-Ion Battery Cathode Materials: Mechanisms and Mitigating Approaches. *Adv. Energy Mater.* **2019**, *9*, 1900551. [[CrossRef](#)]
92. Zhang, C.; Li, T.; Xue, B.; Wu, X.; Li, L.; Guo, Y.; Zhang, L. Synergistic Modification of Ni-Rich Full Concentration Gradient Materials with Enhanced Thermal Stability. *Chem. Eng. J.* **2023**, *451*, 138518. [[CrossRef](#)]
93. Li, W.; Yang, L.; Li, Y.; Chen, Y.; Guo, J.; Zhu, J.; Pan, H.; Xi, X. Ultra-Thin $AlPO_4$ Layer Coated $LiNi_{0.7}Co_{0.15}Mn_{0.15}O_2$ Cathodes with Enhanced High-Voltage and High-Temperature Performance for Lithium-Ion Half/Full Batteries. *Front. Chem.* **2020**, *8*, 597. [[CrossRef](#)]
94. Shen, Y.; Zhang, X.; Wang, L.; Zhang, D.; Bao, D.; Yin, D.; Wang, L.; Cheng, Y.; Huang, G. A Universal Multifunctional Rare Earth Oxide Coating to Stabilize High-Voltage Lithium Layered Oxide Cathodes. *Energy Storage Mater.* **2023**, *56*, 155–164. [[CrossRef](#)]
95. Chen, Z.; Kim, G.T.; Guang, Y.; Bresser, D.; Diemant, T.; Huang, Y.; Copley, M.; Behm, R.J.; Passerini, S.; Shen, Z. Manganese Phosphate Coated $Li[Ni_{0.6}Co_{0.2}Mn_{0.2}]O_2$ Cathode Material: Towards Superior Cycling Stability at Elevated Temperature and High Voltage. *J. Power Sources* **2018**, *402*, 263–271. [[CrossRef](#)]
96. He, X.; Xu, X.; Wang, L.; Du, C.; Cheng, X.; Zuo, P.; Ma, Y.; Yin, G. Enhanced Electrochemical Performance of $LiNi_{0.8}Co_{0.15}Al_{0.05}O_2$ Cathode Material via Li_2TiO_3 Nanoparticles Coating. *J. Electrochem. Soc.* **2019**, *166*, A143. [[CrossRef](#)]
97. Yang, G.; Pan, K.; Lai, F.; Wang, Z.; Chu, Y.; Yang, S.; Han, J.; Wang, H.; Zhang, X.; Li, Q. Integrated Co-Modification of PO_4^{3-} Polyanion Doping and Li_2TiO_3 Coating for Ni-Rich Layered $LiNi_{0.6}Co_{0.2}Mn_{0.2}O_2$ Cathode Material of Lithium-Ion Batteries. *Chem. Eng. J.* **2021**, *421*, 129964. [[CrossRef](#)]

98. Sun, Y.; Liu, Z.; Chen, X.; Yang, X.; Xiang, F.; Lu, W. Enhancing the Stabilities and Electrochemical Performances of $\text{LiNi}_{0.5}\text{Co}_{0.2}\text{Mn}_{0.3}\text{O}_2$ Cathode Material by Simultaneous LiAlO_2 Coating and Al Doping. *Electrochim. Acta* **2021**, *376*, 138038. [[CrossRef](#)]
99. Zhang, J.; Li, Z.; Gao, R.; Hu, Z.; Liu, X. High Rate Capability and Excellent Thermal Stability of Li^+ -Conductive Li_2ZrO_3 -Coated $\text{LiNi}_{1/3}\text{Co}_{1/3}\text{Mn}_{1/3}\text{O}_2$ via a Synchronous Lithiation Strategy. *J. Phys. Chem. C* **2015**, *119*, 20350–20356. [[CrossRef](#)]
100. Gan, Q.; Qin, N.; Wang, Z.; Li, Z.; Zhu, Y.; Li, Y.; Gu, S.; Yuan, H.; Luo, W.; Lu, L.; et al. Revealing Mechanism of Li_3PO_4 Coating Suppressed Surface Oxygen Release for Commercial Ni-Rich Layered Cathodes. *ACS Appl. Energy Mater.* **2020**, *3*, 7445–7455. [[CrossRef](#)]
101. Tang, Z.F.; Wu, R.; Huang, P.F.; Wang, Q.S.; Chen, C.H. Improving the Electrochemical Performance of Ni-Rich Cathode Material $\text{LiNi}_{0.815}\text{Co}_{0.15}\text{Al}_{0.035}\text{O}_2$ by Removing the Lithium Residues and Forming Li_3PO_4 Coating Layer. *J. Alloys Compd.* **2017**, *693*, 1157–1163.
102. Lee, S.W.; Kim, M.S.; Jeong, J.H.; Kim, D.H.; Chung, K.Y.; Roh, K.C.; Kim, K.B. Li_3PO_4 Surface Coating on Ni-Rich $\text{LiNi}_{0.6}\text{Co}_{0.2}\text{Mn}_{0.2}\text{O}_2$ by a Citric Acid Assisted Sol-Gel Method: Improved Thermal Stability and High-Voltage Performance. *J. Power Sources* **2017**, *360*, 206–214. [[CrossRef](#)]
103. Kim, M.Y.; Song, Y.W.; Lim, J.; Park, S.J.; Kang, B.S.; Hong, Y.; Kim, H.S.; Han, J.H. LATP-Coated NCM-811 for High-Temperature Operation of All-Solid Lithium Battery. *Mater. Chem. Phys.* **2022**, *290*, 126644. [[CrossRef](#)]
104. Qian, D.; Xu, B.; Cho, H.M.; Hatsukade, T.; Carroll, K.J.; Meng, Y.S. Lithium Lanthanum Titanium Oxides: A Fast Ionic Conductive Coating for Lithium-Ion Battery Cathodes. *Chem. Mater.* **2012**, *24*, 2744–2751. [[CrossRef](#)]
105. Zhong, Z.; Chen, L.; Zhu, C.; Ren, W.; Kong, L.; Wan, Y. Nano LiFePO_4 Coated Ni Rich Composite as Cathode for Lithium Ion Batteries with High Thermal Ability and Excellent Cycling Performance. *J. Power Sources* **2020**, *464*, 228235. [[CrossRef](#)]
106. Zhu, L.; Yan, T.F.; Jia, D.; Wang, Y.; Wu, Q.; Gu, H.T.; Wu, Y.M.; Tang, W.P. LiFePO_4 -Coated $\text{LiNi}_{0.5}\text{Co}_{0.2}\text{Mn}_{0.3}\text{O}_2$ Cathode Materials with Improved High Voltage Electrochemical Performance and Enhanced Safety for Lithium Ion Pouch Cells. *J. Electrochem. Soc.* **2019**, *166*, A5437. [[CrossRef](#)]
107. Chen, J.; Zhu, L.; Jia, D.; Jiang, X.; Wu, Y.; Hao, Q.; Xia, X.; Ouyang, Y.; Peng, L.; Tang, W.; et al. $\text{LiNi}_{0.8}\text{Co}_{0.15}\text{Al}_{0.05}\text{O}_2$ Cathodes Exhibiting Improved Capacity Retention and Thermal Stability due to a Lithium Iron Phosphate Coating. *Electrochim. Acta* **2019**, *312*, 179–187. [[CrossRef](#)]
108. Duan, J.; Wu, C.; Cao, Y.; Du, K.; Peng, Z.; Hu, G. Enhanced Electrochemical Performance and Thermal Stability of $\text{LiNi}_{0.80}\text{Co}_{0.15}\text{Al}_{0.05}\text{O}_2$ via Nano-Sized LiMnPO_4 Coating. *Electrochim. Acta* **2016**, *221*, 14–22. [[CrossRef](#)]
109. Sun, Y.K.; Myung, S.T.; Park, B.C.; Prakash, J.; Belharouak, I.; Amine, K. High-Energy Cathode Material for Long-Life and Safe Lithium Batteries. *Nat. Mater.* **2009**, *8*, 320–324. [[CrossRef](#)]
110. Sun, Y.K.; Chen, Z.; Noh, H.J.; Lee, D.J.; Jung, H.G.; Ren, Y.; Wang, S.; Yoon, C.S.; Myung, S.T.; Amine, K. Nanostructured High-Energy Cathode Materials for Advanced Lithium Batteries. *Nat. Mater.* **2012**, *11*, 942–947. [[CrossRef](#)] [[PubMed](#)]
111. Kim, U.H.; Ryu, H.H.; Kim, J.H.; Mücke, R.; Kaghazchi, P.; Yoon, C.S.; Sun, Y.K. Microstructure-Controlled Ni-Rich Cathode Material by Microscale Compositional Partition for Next-Generation Electric Vehicles. *Adv. Energy Mater.* **2019**, *9*, 1803902. [[CrossRef](#)]
112. Xu, X.; Xiang, L.; Wang, L.; Jian, J.; Du, C.; He, X.; Huo, H.; Cheng, X.; Yin, G. Progressive Concentration Gradient Nickel-Rich Oxide Cathode Material for High-Energy and Long-Life Lithium-Ion Batteries. *J. Mater. Chem. A* **2019**, *7*, 7728–7735. [[CrossRef](#)]
113. Shi, J.L.; Qi, R.; Zhang, X.D.; Wang, P.F.; Wang, P.F.; Fu, W.G.; Yin, Y.X.; Xu, J.; Wan, L.J.; Guo, Y.G. High-Thermal-and Air-Stability Cathode Material with Concentration-Gradient Buffer for Li-Ion Batteries. *ACS Appl. Mater. Interfaces* **2017**, *9*, 42829–42835. [[CrossRef](#)] [[PubMed](#)]
114. Mo, Y.; Guo, L.; Jin, H.; Du, B.; Cao, B.; Chen, Y.; Chen, Y. Building Nickel-Rich Cathodes with Large Concentration Gradient for High Performance Lithium-Ion Batteries. *J. Power Sources* **2020**, *468*, 228405. [[CrossRef](#)]
115. Park, G.T.; Ryu, H.H.; Noh, T.C.; Kang, G.C.; Sun, Y.K. Microstructure-Optimized Concentration-Gradient NCM Cathode for Long-Life Li-Ion Batteries. *Mater. Today* **2022**, *52*, 9–18. [[CrossRef](#)]
116. Zeng, X.; Jian, T.; Lu, Y.; Yang, L.; Ma, W.; Yang, Y.; Zhu, J.; Huang, C.; Dai, S.; Xi, X. Enhancing High-Temperature and High-Voltage Performances of Single-Crystal $\text{LiNi}_{0.5}\text{Co}_{0.2}\text{Mn}_{0.3}\text{O}_2$ Cathodes Through a $\text{LiBO}_2/\text{LiAlO}_2$ Dual-Modification Strategy. *ACS Sustain. Chem. Eng.* **2020**, *8*, 6293–6304. [[CrossRef](#)]
117. Ma, Y.; Xu, M.; Zhang, J.; Liu, R.; Wang, Y.; Xiao, H.; Huang, Y.; Yuan, G. Improving Electrochemical Performance of Ni-Rich $\text{LiNi}_{0.8}\text{Co}_{0.1}\text{Mn}_{0.1}\text{O}_2$ Cathode for Li-Ion Batteries by Dual-Conductive Coating Layer of PPy and LiAlO_2 . *J. Alloys Compd.* **2020**, *848*, 156387. [[CrossRef](#)]
118. Cao, G.; Zhang, M.; Zhang, L.; Wang, Y.; Yan, Y.; Li, Z.; Sun, X.; Zhang, D. Excellent High-Rate Cyclic Performance of $\text{LiNi}_{0.8}\text{Co}_{0.1}\text{Mn}_{0.1}\text{O}_2$ Cathodes via Dual $\text{Li}_2\text{SiO}_3/\text{PPy}$ Coating. *J. Alloys Compd.* **2022**, *938*, 168575. [[CrossRef](#)]
119. Wei, Z.; Liang, C.; Jiang, L.; Wang, L.; Cheng, S.; Peng, Q.; Feng, L.; Zhang, W.; Sun, J.; Wang, Q. In-Depth Study on Diffusion of Oxygen Vacancies in $\text{Li}(\text{Ni}_x\text{Co}_y\text{Mn}_z)\text{O}_2$ Cathode Materials Under Thermal Induction. *Energy Storage Mater.* **2022**, *47*, 51–60. [[CrossRef](#)]
120. Ryu, H.H.; Park, N.Y.; Seo, J.H.; Yu, Y.S.; Sharma, M.; Mücke, R.; Kaghazchi, P.; Yoon, C.S.; Sun, Y.K. A Highly Stabilized Ni-Rich NCA Cathode for High-Energy Lithium-Ion Batteries. *Mater. Today* **2020**, *36*, 73–82. [[CrossRef](#)]
121. Kim, Y.S.; Kim, J.H.; Sun, Y.K.; Yoon, C.S. Evolution of a Radially Aligned Microstructure in Boron-Doped $\text{Li}[\text{Ni}_{0.95}\text{Co}_{0.04}\text{Al}_{0.01}]\text{O}_2$ Cathode Particles. *ACS Appl. Mater. Interfaces* **2022**, *14*, 17500–17508. [[CrossRef](#)] [[PubMed](#)]

122. Kim, U.H.; Park, G.T.; Son, B.K.; Nam, G.W.; Liu, J.; Kuo, L.Y.; Kaghazchi, P.; Yoon, C.S.; Sun, Y.K. Heuristic Solution for Achieving Long-Term Cycle Stability for Ni-Rich Layered Cathodes at Full Depth of Discharge. *Nat. Energy* **2020**, *5*, 860–869. [[CrossRef](#)]
123. Nguyen, T.T.; Kim, U.H.; Yoon, C.S.; Sun, Y.K. Enhanced Cycling Stability of Sn-Doped $\text{Li}[\text{Ni}_{0.90}\text{Co}_{0.05}\text{Mn}_{0.05}]\text{O}_2$ via Optimization of Particle Shape and Orientation. *Chem. Eng. J.* **2021**, *405*, 126887. [[CrossRef](#)]
124. Du, B.; Mo, Y.; Jin, H.; Li, X.; Qu, Y.; Li, D.; Cao, B.; Jia, X.; Lu, Y.; Chen, Y. Radially Microstructural Design of $\text{LiNi}_{0.8}\text{Co}_{0.1}\text{Mn}_{0.1}\text{O}_2$ Cathode Material toward Long-Term Cyclability and High Rate Capability at High Voltage. *ACS Appl. Energy Mater.* **2020**, *3*, 6657–6669. [[CrossRef](#)]
125. Harlow, J.E.; Ma, X.; Li, J.; Logan, E.; Liu, Y.; Zhang, N.; Ma, L.; Glazier, S.L.; Cormier, M.M.E.; Genovese, M.; et al. A Wide Range of Testing Results on an Excellent Lithium-Ion Cell Chemistry to be Used as Benchmarks for New Battery Technologies. *J. Electrochem. Soc.* **2019**, *166*, A3031–A3044. [[CrossRef](#)]
126. Li, J.; Cameron, A.R.; Li, H.; Glazier, S.; Xiong, D.; Chatzidakis, M.; Allen, J.; Botton, G.A.; Dahn, J.R. Comparison of Single Crystal and Polycrystalline $\text{LiNi}_{0.5}\text{Mn}_{0.3}\text{Co}_{0.2}\text{O}_2$ Positive Electrode Materials for High Voltage Li-Ion Cells. *J. Electrochem. Soc.* **2017**, *164*, A1534. [[CrossRef](#)]
127. Weber, R.; Fell, C.R.; Dahn, J.R.; Hy, S. Operando X-ray Diffraction Study of Polycrystalline and Single-Crystal $\text{Li}_x\text{Ni}_{0.5}\text{Mn}_{0.3}\text{Co}_{0.2}\text{O}_2$. *J. Electrochem. Soc.* **2017**, *164*, A2992–A2999. [[CrossRef](#)]
128. Liu, A.; Zhang, N.; Stark, J.E.; Arab, P.; Li, H.; Dahn, J.R. Synthesis of Co-free Ni-rich Single Crystal Positive Electrode Materials for Lithium Ion Batteries: Part i. Two-Step Lithiation Method for Al-or Mg-doped LiNiO_2 . *J. Electrochem. Soc.* **2021**, *168*, 040531. [[CrossRef](#)]
129. Li, J.; Li, H.; Stone, W.; Glazier, S.; Dahn, J.R. Development of Electrolytes for Single Crystal NMC532/Artificial Graphite Cells with Long Lifetime. *J. Electrochem. Soc.* **2018**, *165*, A626–A635. [[CrossRef](#)]
130. Kong, X.; Zhang, Y.; Li, J.; Yang, H.; Dai, P.; Zeng, J.; Zhao, J. Single-Crystal Structure Helps Enhance the Thermal Performance of Ni-Rich Layered Cathode Materials for Lithium-Ion Batteries. *Chem. Eng. J.* **2022**, *434*, 134638. [[CrossRef](#)]
131. Huang, B.; Wang, M.; Zhang, X.; Zhao, Z.; Chen, L.; Gu, Y. Synergistic coupling effect of single crystal morphology and precursor treatment of Ni-Rich cathode materials. *J. Alloys Compd.* **2020**, *830*, 154619. [[CrossRef](#)]
132. Pang, P.; Tan, X.; Wang, Z.; Cai, Z.; Nan, J.; Xing, Z.; Li, H. Crack-Free Single-Crystal $\text{LiNi}_{0.83}\text{Co}_{0.10}\text{Mn}_{0.07}\text{O}_2$ as Cycling/Thermal Stable Cathode Materials for High-Voltage Lithium-Ion Batteries. *Electrochim. Acta* **2021**, *365*, 137380. [[CrossRef](#)]
133. Zhong, Z.; Chen, L.; Huang, S.; Shang, W.; Kong, L.; Sun, M.; Chen, L.; Ren, W. Single-Crystal $\text{LiNi}_{0.5}\text{Co}_{0.2}\text{Mn}_{0.3}\text{O}_2$: A High Thermal and Cycling Stable Cathodes for Lithium-Ion Batteries. *J. Mater. Sci.* **2020**, *55*, 2913–2922. [[CrossRef](#)]
134. Liu, G.; Li, M.; Wu, N.; Cui, L.; Huang, X.; Liu, X.; Zhao, Y.; Chen, H.; Yuan, W.; Bai, Y. Single-Crystalline Particles: An Effective Way to Ameliorate the Intragranular Cracking, Thermal Stability, and Capacity Fading of the $\text{LiNi}_{0.6}\text{Co}_{0.2}\text{Mn}_{0.2}\text{O}_2$ Electrodes. *J. Electrochem. Soc.* **2018**, *165*, A3040. [[CrossRef](#)]
135. Ge, M.; Wi, S.; Liu, X.; Bai, J.; Ehrlich, S.; Lu, D.; Lee, W.K.; Chen, Z.H.; Wang, F. Kinetic Limitations in Single-Crystal High-Nickel Cathodes. *Angew. Chem. Int. Ed.* **2021**, *60*, 17350–17355. [[CrossRef](#)]
136. Bi, Y.; Tao, J.; Wu, Y.; Li, L.; Xu, Y.; Hu, E.; Wu, B.; Hu, J.; Wang, C.; Zhang, J.; et al. Reversible planar gliding and microcracking in a single-crystalline Ni-rich cathode. *Science* **2020**, *370*, 1313–1317. [[CrossRef](#)] [[PubMed](#)]
137. Kim, U.H.; Lee, E.J.; Yoon, C.S.; Myung, S.T.; Sun, Y.K. Compositionally Graded Cathode Material with Long-Term Cycling Stability for Electric Vehicles Application. *Adv. Energy Mater.* **2016**, *6*, 1601417. [[CrossRef](#)]
138. Feng, Z.; Rajagopalan, R.; Zhang, S.; Sun, D.; Tang, Y.; Ren, Y.; Wang, H. A Three in One Strategy to Achieve Zirconium Doping, Boron Doping, and Interfacial Coating for Stable $\text{LiNi}_{0.8}\text{Co}_{0.1}\text{Mn}_{0.1}\text{O}_2$ Cathode. *Adv. Sci.* **2021**, *8*, 2001809. [[CrossRef](#)]
139. Zhang, B.; Shen, J.; Wang, Q.; Hu, C.; Luo, B.; Liu, Y.; Xiao, Z.; Ou, X. Boosting High-Voltage and Ultralong-Cycling Performance of Single-Crystal $\text{LiNi}_{0.5}\text{Co}_{0.2}\text{Mn}_{0.3}\text{O}_2$ Cathode Materials via Three-in-One Modification. *Energy Environ. Mater.* **2023**, *6*, e12270. [[CrossRef](#)]
140. Bao, W.; Qian, G.; Zhao, L.; Yu, Y.; Su, L.; Cai, X.; Zhao, H.; Zuo, Y.; Zhang, Y.; Li, H.; et al. Simultaneous Enhancement of Interfacial Stability and Kinetics of Single-Crystal $\text{LiNi}_{0.6}\text{Mn}_{0.2}\text{Co}_{0.2}\text{O}_2$ Through Optimized Surface Coating and Doping. *Nano Lett.* **2020**, *20*, 8832–8840. [[CrossRef](#)]
141. Zhou, G.; Wei, Y.; Li, H.; Wang, C.; Huang, X.; Yang, D. Al_2O_3 -Coated, Single Crystal Zr/Y co-Doped High-Ni NCM Cathode Materials for High-Performance Lithium-Ion Batteries. *Part. Part. Syst. Charact.* **2022**, *39*, 2200061. [[CrossRef](#)]
142. Shen, J.; Deng, D.; Li, X.; Zhang, B.; Xiao, Z.; Hu, C.; Yan, X.; Ou, X. Realizing Ultrahigh-Voltage Performance of Single-Crystalline $\text{LiNi}_{0.55}\text{Co}_{0.15}\text{Mn}_{0.3}\text{O}_2$ Cathode Materials by Simultaneous Zr-Doping and B_2O_3 -Coating. *J. Alloys Compd.* **2022**, *903*, 163999. [[CrossRef](#)]
143. Fan, X.M.; Huang, Y.D.; Wei, H.X.; Tang, L.B.; He, Z.J.; Yan, C.; Mao, J.; Dai, K.H.; Zheng, J.C. Surface Modification Engineering Enabling 4.6 V Single-Crystalline Ni-Rich Cathode with Superior Long-Term Cyclability. *Adv. Funct. Mater.* **2022**, *32*, 2109421. [[CrossRef](#)]
144. Han, Y.; Xu, J.; Wang, W.; Long, F.; Qu, Q.; Wang, Y.; Zheng, H. Implanting an Electrolyte Additive on a Single Crystal Ni-Rich Cathode Surface for Improved Cycleability and Safety. *J. Mater. Chem. A* **2020**, *8*, 24579–24589. [[CrossRef](#)]
145. Lim, D.A.; Shin, Y.K.; Seok, J.H.; Hong, D.; Ahn, K.H.; Lee, C.H.; Kim, D.W. Cathode Electrolyte Interphase-Forming Additive for Improving Cycling Performance and Thermal Stability of Ni-Rich $\text{LiNi}_x\text{Co}_y\text{Mn}_{1-x-y}\text{O}_2$ Cathode Materials. *ACS Appl. Mater. Interfaces* **2022**, *14*, 54688–54697. [[CrossRef](#)] [[PubMed](#)]

146. Jiang, L.; Wang, Q.; Sun, J. Electrochemical Performance and Thermal Stability Analysis of $\text{LiNi}_x\text{Co}_y\text{Mn}_z\text{O}_2$ Cathode Based on a Composite Safety Electrolyte. *J. Hazard. Mater.* **2018**, *351*, 260–269. [[CrossRef](#)] [[PubMed](#)]
147. Yu, J.; Zhou, P.; Jiang, S. Experimental Study on the Effect of Electrolyte Flame Retardant Additives on the Nail Penetration Safety of Lithium-Ion Battery. *Fire Sci. Technol.* **2022**, *41*, 1209.
148. Li, Y.; An, Y.; Tian, Y.; Fei, H.; Xiong, S.; Qian, Y.; Feng, J. Stable and Safe Lithium Metal Batteries with Ni-Rich Cathodes Enabled by a High Efficiency Flame Retardant Additive. *J. Electrochem. Soc.* **2019**, *166*, A2736. [[CrossRef](#)]
149. An, K.; Tran, Y.H.T.; Kwak, S.; Han, J.; Song, S.W. Design of Fire-Resistant Liquid Electrolyte Formulation for Safe and Long-Cycled Lithium-Ion Batteries. *Adv. Funct. Mater.* **2021**, *31*, 2106102. [[CrossRef](#)]
150. Kim, A.Y.; Strauss, F.; Bartsch, T.; Teo, J.H.; Hatsukade, T.; Mazilkin, A.; Janek, J.; Hartmann, P.; Brezesinski, T. Stabilizing Effect of a Hybrid Surface Coating on a Ni-Rich NCM Cathode Material in All-Solid-State Batteries. *Chem. Mater.* **2019**, *31*, 9664–9672. [[CrossRef](#)]
151. Wang, S.; Fang, R.; Li, Y.; Liu, Y.; Xin, C.; Richter, F.H.; Nan, C.W. Interfacial Challenges for All-Solid-State Batteries Based on Sulfide Solid Electrolytes. *J. Mater.* **2021**, *7*, 209–218. [[CrossRef](#)]
152. Vadhva, P.; Hu, J.; Johnson, M.J.; Stocker, R.; Braglia, M.; Brett, D.J.; Rettie, A.J. Electrochemical Impedance Spectroscopy for All-Solid-State Batteries: Theory, Methods and Future Outlook. *ChemElectroChem* **2021**, *8*, 1930–1947. [[CrossRef](#)]
153. Meng, F.; Gao, J.; Zhang, M.; Li, D.; Liu, X. Enhanced Safety Performance of Automotive Lithium-Ion Batteries with Al_2O_3 -Coated Non-Woven Separator. *Batter. Supercaps* **2021**, *4*, 146–151. [[CrossRef](#)]
154. Kim, P.S.; Le Mong, A.; Kim, D. Thermal, Mechanical, and Electrochemical Stability Enhancement of Al_2O_3 Coated Polypropylene/polyethylene/polypropylene Separator via Poly (vinylidene fluoride)-Poly (ethoxylated pentaerythritol tetraacrylate) Semi-Interpenetrating Network Binder. *J. Membr. Sci.* **2020**, *612*, 118481. [[CrossRef](#)]
155. Pham, H.Q.; Lee, H.Y.; Hwang, E.H.; Kwon, Y.G.; Song, S.W. Non-Flammable Organic Liquid Electrolyte for High-Safety and High-Energy Density Li-Ion Batteries. *J. Power Sources* **2018**, *404*, 13–19. [[CrossRef](#)]
156. Pham, H.Q.; Kim, G.; Jung, H.M.; Song, S.W. Fluorinated Polyimide as a Novel High-Voltage Binder for High-Capacity Cathode of Lithium-Ion Batteries. *Adv. Funct. Mater.* **2018**, *28*, 1704690. [[CrossRef](#)]
157. McKerracher, R.D.; Guzman-Guemez, J.; Wills, R.G.; Sharkh, S.M.; Kramer, D. Advances in Prevention of Thermal Runaway in Lithium-Ion Batteries. *Adv. Energy Sustain. Res.* **2021**, *2*, 2000059. [[CrossRef](#)]
158. Zhang, X.; Zhang, C.; Li, H.; Cao, Y.; Yang, H.; Ai, X. Reversible Temperature-Responsive Cathode for Thermal Protection of Lithium-Ion Batteries. *ACS Appl. Energy Mater.* **2022**, *5*, 5236–5244. [[CrossRef](#)]

Disclaimer/Publisher’s Note: The statements, opinions and data contained in all publications are solely those of the individual author(s) and contributor(s) and not of MDPI and/or the editor(s). MDPI and/or the editor(s) disclaim responsibility for any injury to people or property resulting from any ideas, methods, instructions or products referred to in the content.